NATURAL RESOURCES

Geologic Map of the Forks 1:100,000 Quadrangle, Washington

compiled by
Wendy J. Gerstel and
William S. Lingley, Jr.

Zircon fission-track minimum ages
by R. J. Stewart

WASHINGTON
DIVISION OF GEOLOGY
AND EARTH RESOURCES

Open File Report 2000-4
October 2000

Location of quadrangle

WASHINGTON STATE DEPARTMENT OF
Natural Resources
Jennifer M. Belcher - Commissioner of Public Lands

Geologic Map of the Forks 1:100,000 Quadrangle, Washington

compiled by
Wendy J. Gerstel and
William S. Lingley, Jr.

Zircon fission-track minimum ages
by R. J. Stewart, University of Washington

WASHINGTON
DIVISION OF GEOLOGY
AND EARTH RESOURCES

Open File Report 2000-4
October 2000

Produced in cooperation with the U.S. Geological Survey
National Cooperative Geologic Mapping Program
Agreement Number 98HQAG2062

WASHINGTON STATE DEPARTMENT OF
Natural Resources
Jennifer M. Belcher - Commissioner of Public Lands

Contents

APPENDIX

ILLUSTRATIONS

TABLE

PLATES *(accompany text)*

Geologic Map of the Forks 1:100,000 Quadrangle, Washington

Compiled by
Wendy J. Gerstel and William S. Lingley, Jr.
Washington Division of Geology and Earth Resources
PO Box 47007; Olympia, WA 98504-7007
wendy.gerstel@wadnr.gov; william.lingley@wadnr.gov

With new zircon fission-track minimum ages
by R. J. Stewart
University of Washington

INTRODUCTION

This report describes a compilation of geologic mapping of the Forks 1:100,000 quadrangle, which covers the west-central portion of the Olympic Peninsula, Washington (Plate 1). It is one of 15 whole or partial 1:100,000-scale quadrangles composing the northwest quadrant of the state geologic map, which is being compiled at 1:250,000 (Fig. 1) by the Washington Division of Geology and Earth Resources (DGER). Users may obtain copies of the geographic information system (GIS) database of the Forks quadrangle from DGER by calling (360) 902-1450 or e-mailing geology@wadnr.gov.

Physiographically, the Forks quadrangle encompasses the lower western slopes of the Olympic Mountains and extends westward to the Pacific Ocean. Major rivers flowing westward through the area include, from north to south, the Dickey, Quillayute, Hoh, and Queets. The Quillayute River is formed by the confluence of the Sol Duc, Sitkum, Calawah, and Bogachiel Rivers. Matheny Creek and the Salmon, Solleks, and Clearwater Rivers are some of the larger tributaries of the Queets River. The Snahapish River is the main tributary of the Clearwater River. Smaller streams within the coastal foothills include (from the north): Goodman, Mosquito, Nolan, Christmas, Miller, Shale, and Kalaloch Creeks.

The higher foothills of the southern portions of the Forks quadrangle consist of heavily forested ridges and intervening valleys that trend and diminish in elevation westward. Relevant intervening ridges, named for their high points, are (from the north): Elk–Rugged Ridge, Geodetic Hill, Huelsdonk Ridge, Mount Octopus, Kloochman Rock, and Matheny Ridge.

Variation in the angle and rate of convergence of the Juan de Fuca plate with the North America plate is responsible for the distinct geology of the Olympic Peninsula (Babcock and others, 1994; Brandon and Calderwood, 1990; Brandon and Vance, 1992). The peninsula is underlain by sequences of Tertiary marine and paralic sediments, volcanogenic rocks, and sediments deposited in bathyal environments from sandy debris flows (Plate 2). In the eastern and central portions of the peninsula, these are all folded and uplifted into a broad, ENE-plunging anticline (Tabor, 1975). In the Forks quadrangle, these same rocks form an east-dipping, regional homocline that is complexly folded and faulted on smaller scales. Southwest-verging thrust faults dominate regional structure. The Hoh and Queets Rivers, as well as the glaciers that periodically occupied their valleys, follow the traces of northeast-trending fault zones.

Much of the quadrangle is covered by Quaternary sediments, mostly deposited from alpine glaciers. The western parts of most drainages dissect early Wisconsinan glacial deposits forming some of the higher lowland terraces. In compiling the mapping, we have attempted to give equal attention to the Tertiary bedrock and Quaternary sediments, contributing new information on age correlations for younger geologic materials and climatic events on the peninsula.

Figure 2 identifies primary sources of data used to compile this map. (See Fig. 3 for geographic features referred to in the text and the location of 7.5-minute quadrangles.)

PREVIOUS WORK

Quaternary Deposits

Reagan (1909) provided one of the first discussions of past glacial activity in the Olympic Mountains, but until recently, most geologic maps of the Olympic Peninsula featured bedrock stratigraphy and structure. Quaternary deposits were shown mostly

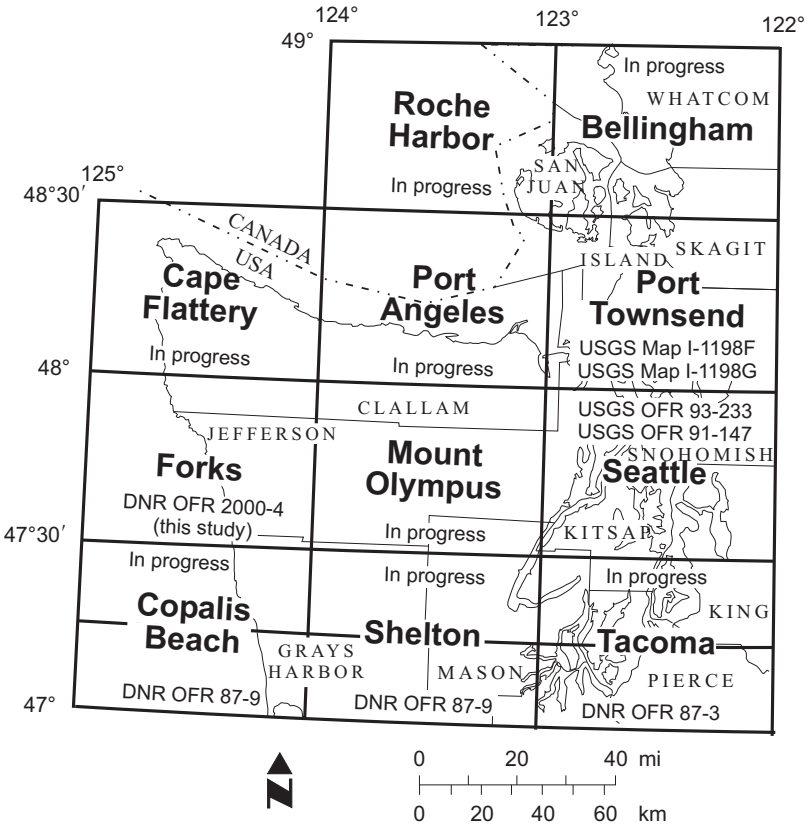

Figure 1. Map showing 30- by 60-minute (1:100,000-scale) quadrangles in the northwest quadrant of Washington. Bold type and boxes are quadrangles. Lighter lines and type indicate counties. All map numbers with the prefix DNR are Division of Geology and Earth Resources publications. U.S. Geological Survey (USGS) maps and open-file reports (OFR) can be obtained from the USGS.

where they obscured the bedrock, and then only as two or three units defined by broad-scope chronologic assignment and origin.

Crandell (1964, 1965) and Heusser (1964, 1969, 1973a,b, 1978) were among the earliest workers to attempt to establish a chronology for Quaternary deposits on the Olympic Peninsula. Their conclusions were based on radiocarbon dating of peats, relative soil development, and relative geographic and stratigraphic position of deposits. Crandell (1965) presented an overview of the entire peninsula and suggested correlations with Puget Sound and Cascade glacial stratigraphy. He assigned the oldest deposits to the Salmon Springs Glaciation; the next youngest to the Evans Creek Stade of the Fraser Glaciation at 25,000 to 20,000 yr B.P. or older; and the youngest to the Vashon Stade of the Fraser Glaciation at 20,000 to about 12,000 yr B.P. The name 'Salmon Springs' was first applied to Puget Lowland glacial deposits laid down just before the Vashon. These were thought to date to about 36,000 yr B.P. Subsequently, the type locality for the Salmon Springs has been determined to be much older (Easterbrook and others, 1981), causing confusion and inconsistencies in the literature. Dates from a limited number of samples were extrapolated throughout the valleys of the peninsula.

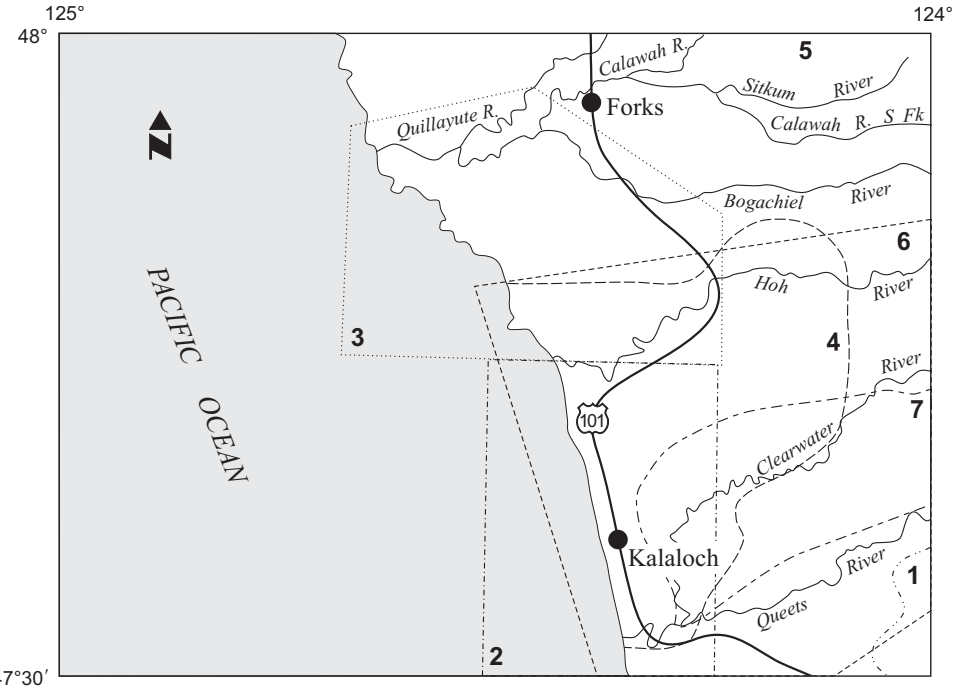

Figure 2. Map showing primary sources of geological mapping for the Forks 1:100,000 quadrangle. **1**, Lingley and others, 1996 (scale 1:62,500); **2**, Rau, 1975 (scale 1:24,000); **3**, Rau, 1979 (scale 1:24,000); **4**, Stewart, 1970 (scale 1:62,500); **5**, Tabor and Cady, 1978a (scale 1:200,000); **6**, Thackray, 1996 (scale 1:100,000); **7**, Wegmann, 1999 (scale 1:12,000). Unpublished mapping: Lingley (in press); C. Finn (USGS, written commun., 1989). Numbers are shown inside the boundaries of the map areas.

Heusser (1964, 1969, 1973a,b, 1974, 1978), concentrating his studies in the Hoh and Bogachiel drainages, noted evidence for at least two major glacial advances—around 18,000 yr B.P. and prior to 30,000 yr B.P. The earlier advance he also correlated to the 'Salmon Springs' glaciation. The confusion in the stratigraphic nomenclature persisted, because the Salmon Springs had been assigned ages from pre-Wisconsinan, probably older than about 140,000 years ago (Crandell, 1964), to pre-Olympia interglacial, about 36,000 years ago (Easterbrook and others, 1967).

Rau (1975, 1979) broke out two Quaternary units—undivided alpine glacial deposits and alluvium—providing limited information on the distribution and timing of glaciations in the area. Rau (1973, 1980) recognized the significance of raised marine terraces along the central coast, discussing their relationship to older glaciations and rates of coastal retreat and tectonic deformation.

Long (1975, 1976) compiled field observations of Quaternary deposits of the entire Olympic Peninsula. This mapping, collected over many years of work with the U.S. Forest Service, encompassed most of the valleys radiating from the Olympic Mountains. Long's unpublished maps and text also applied stratigraphic correlations developed in the Cascade Range to the deposits of the peninsula and were based on the age determinations suggested by Crandell and other Cascade mappers. This forestalled development of a locally derived Quaternary stratigraphy and made age assignments on the peninsula difficult and unreliable.

Interpretations based on Cascade nomenclature and timing perpetuated the concept of synchronous alpine glaciation throughout North America. However, recent work on the peninsula by Thackray (1996) and a review by Gillespie and Molnar (1995) of studies on alpine glacial stratigraphy throughout the world suggest that alpine glaciation in the Olympic Mountains may have been asynchronous with respect to glaciations in other North American mountain ranges and with respect to continental advances. The Olympic Mountains glaciers were probably particularly responsive to small climatic changes.

Thackray (1996), working in the Hoh and Queets drainages, began establishing a chronology of glacial advances and retreats specific to the Olympic Peninsula. Based on detailed radiocarbon dating, his stratigraphy shows a sequence of glacial advances unique in timing to the Olympic Peninsula and supports the hypothesis of asynchronous glaciations in North America.

Thackray, mapping landforms, defined at least four major glacial advances, some including minor readvances, with terminal positions delineated by moraine locations. Thackray's nomenclature for the Hoh and Queets drainages included (from older to younger): the Wolf Creek advance (inferred to be older than 780,000 years based on reversely magnetized glaciolacustrine and glaciofluvial sediments); the Whale Creek advance (~130,000–180,000[?] yr B.P.); the Lyman Rapids advance (~55,000–110,000 yr B.P.); three Hoh Oxbow advances (~20,000–39,000 yr B.P.); and two Twin Creeks advances (~17,000–19,000 yr B.P. and an undated later readvance). An attempt to correlate this sequence to mapping by Moore (1965) met with limited success.

In a recent paper on the stratigraphy and vegetation of the Humptulips drainage, located within the Copalis Beach 1:100,000-scale quadrangle to the south (Logan, in progress), Heusser and others (1999) suggested glacial advances occurring during oxygen-isotope stage 5a (~60,000 yr B.P.) and several times each during stages 4, 3, and 2 (infinite radiocarbon ages,

~30,000–40,000 yr B.P., and 18,440–24,600 yr B.P., respectively). This temporal framework could easily incorporate the glacial advances suggested by Thackray (1996).

Through detailed radiocarbon dating of organic detritus extracted from terrace deposits, Wegmann (1999) substantiated age estimates made by Thackray and Pazzaglia (1994), Pazzaglia and Brandon (1996), and Thackray (1996) on outwash and alluvial sequences in the Snahapish valley. All three studies agree that only the outwash from pre-Fraser glaciations, best correlated to Thackray's Lyman Rapids drift (unit Qapo on this map) and older glaciations, was deposited into the Snahapish valley and transported down the Clearwater River. The younger, Fraser-age outwash (unit Qao), correlated to Thackray's (1996) Hoh Oxbow glaciation, did not reach the Snahapish valley.

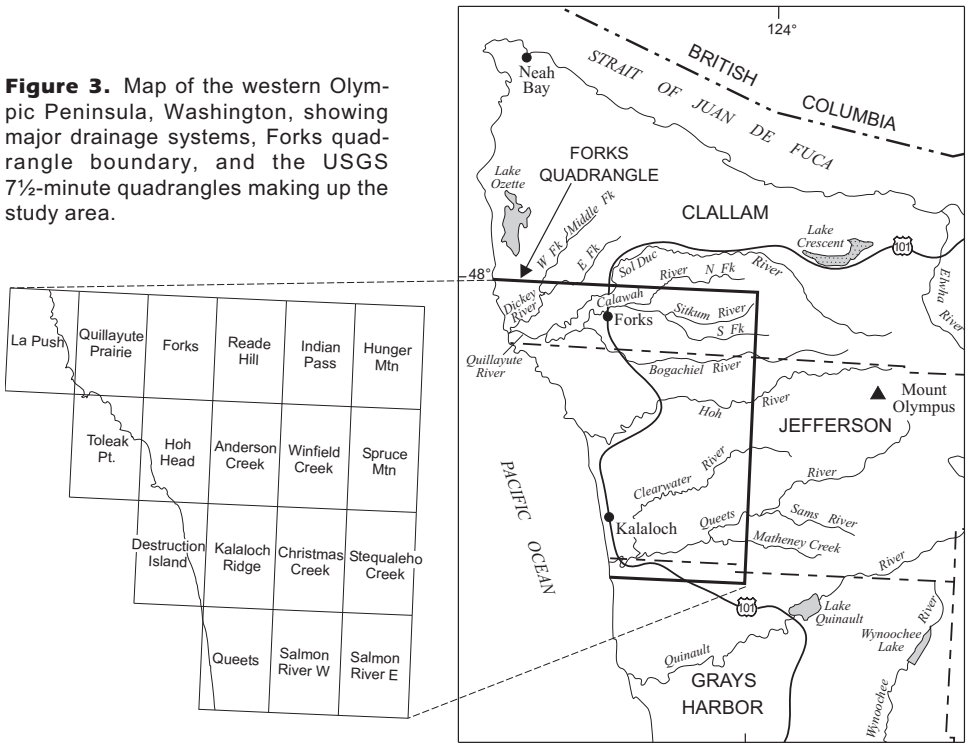

Figure 3. Map of the western Olympic Peninsula, Washington, showing major drainage systems, Forks quadrangle boundary, and the USGS 7½-minute quadrangles making up the study area.

Landslides are a common and significant feature on the Olympic Peninsula. Several studies have compiled inventories of both shallow and deep-seated landslides (Fiksdal and Brunengo, 1980; Shaw, 1995; Dieu and Shelmerdine, 1997; Gerstel, 1999; Lingley, in press). In an effort to characterize shallow landslides and develop models for prediction, Shaw and Vaugeois (1999 and references within) did a comparative study of existing models and slope-rating systems. Only deep-seated landslides, those transferred from the digitally based inventory of Gerstel (1999 and references within), are shown on this map.

Tertiary Rocks

In his entertaining account of fieldwork in the Forks quadrangle, Reagan (1909) described the geology with surprising accuracy, considering only two wagon roads crossed the western Olympic Peninsula at that time. He recognized the major northeast-trending Hoh River fault that controls the Hoh River valley and described regional stratigraphy.

In 1916, Weaver published the first geologic map covering the Forks 1:100,000 quadrangle and defined the 'Hoh Formation', describing banded and laminated sandstones containing slate rip-up clasts. Palmer (1927b) assigned a Miocene to Oligocene age to the Hoh formation based on mollusks and extended its boundary eastward to cover most of the interior of the Olympic Peninsula.

Glover (1940a) named the Brown's Point Formation[1] from a type locality directly north of Kalaloch and noted that the rocks were dissimilar to adjacent mélanges and broken formations. These rocks were included in the Hoh lithic assemblage of Rau (1973).

Stewart (1970) produced the first regional map showing structure and stratigraphy in the interior of the Forks quadrangle. He recognized that the major river valleys issuing from the Olympic Mountains are controlled by northeast-trending faults with wide shear zones containing phacoids of sandstone, conglomerate, and volcanic rocks. He mapped the northwest-trending Salmon River and Huelsdonk shear zones and interpreted these as southwest-verging thrust faults.

Rau (1975, 1979) produced 1:62,500-scale maps of coastal areas based on detailed foraminiferal chronostratigraphy and on the lithostratigraphic scheme also used herein. Rau (1973, 1980) also produced two excellent layperson's bulletins on the geology of the Olympic coast, which outline details of structure, Pleistocene stratigraphy, and uplift history.

Tabor and Cady (1978a) compiled all existing mapping and new structural data in the eastern part of the Forks quadrangle to produce the first detailed map of the Olympic Peninsula. This map is based on lithostratigraphy and sedimentary structures that were used to separate large packets of massive graywacke and thin-bedded finer siliciclastic rocks into lithic assemblages.

Unpublished mapping by Lingley and others (1996) and Richard Stewart (Univ. of Wash., written commun., 1998) helped complete the eastern part of the Forks 1:100,000 quadrangle. A compilation of biostratigraphic age determinations and new zircon fission-track minimum ages, shown in part on Plate 1 and in Appendix 1, was especially useful in preparing this map and the associated GIS database.

Tectonic History

The tectonic history of the Olympic Peninsula is outlined in Tabor (1975), Tabor and Cady (1978b), Snavely (1987), Brandon and Calderwood (1990), Boyer and Lingley (1991, 1994), Brandon and Vance (1992), and Thackray (1998). Rau (1973) and Rau and Grocock (1974) identified piercement structures, such as the Duck Creek diapir. Orange (1990) and Orange and others (1993) performed detailed mapping along the coast to elucidate its structural history. Brown and Orange (1993) developed criteria for distinguishing between shear zone mélanges (including mélanges on thrust faults) and diapiric mélanges.

Stewart (1974), Tabor and Cady (1978a), Orange and others (1993), and Orange and Underwood (1995) described a gener-

[1] This name for these Miocene rocks was not used extensively. Thackray (1998) used the name 'Browns Point formation' for Pleistocene peat, clay, and silt that overlie Glover's Miocene rocks.

ally eastward-increasing progression of diagenesis and zeolite-facies metamorphism. Facies analyses of the sedimentary section within the study area include Koch (1968), Grady (1985), and Lingley (1995). Grady described Bouma sequences near Brown's Point, whereas Lingley observed that much of the section can be divided into submarine channel fill sequences separated by levee and overbank deposits.

Palmer (1927a), Rau and McFarland (1982), McFarland (1983), Grady (1985), Kvenvolden and others (1989a,b), Snavely and Kvenvolden (1989), and Palmer and Lingley (1989) describe the petroleum geology of the area.

LITHIC ASSEMBLAGES AND MAJOR STRUCTURAL SHEETS

Rau (1973, 1975, 1979), Tabor and Cady (1978a,b), and Snavely and others (1993) grouped the rocks in the Forks quadrangle and surrounding areas into lithic assemblages or, in the case of Snavely and others, terranes. These lithic assemblages and terranes are based on strong similarities in biofacies and lithofacies that facilitate mapping. Subsequent work (Lingley, 1995) and new zircon fission-track minimum ages reported herein support the positions of contacts and choices of lithic assemblages used by these authors.

The Hoh lithic assemblage, for example, is characterized by well-developed early to middle Miocene deep-water microfauna, lithic sandstones, reddish-yellow-weathering thin-bedded siliciclastic rhythmites, and both Bouma sequences (Bouma and Brouwer, 1964) and submarine channel-fill/interdistributary deposits. Eocene fauna within the Hoh lithic assemblage are present only in samples from shear or mélange zones. The Western Olympic lithic assemblage of Tabor and Cady (1978a,b) is characterized by mostly Oligocene and Eocene ages, thick well-indurated multistory sandstones separated by laminated sandstone and siltstone couplets, and an absence of mid-fan facies. In the northern part of the Forks quadrangle, the Western Olympic lithic assemblage has been remapped as the Lake Ozette–Calawah Ridge block of Snavely and others (1993), a unit characterized by Eocene medium- to very thick-bedded olive gray sandstone and siltstone.

All available data are consistent with development of the Olympic subduction complex as a southwestward-younging thrust belt (Silver, 1972; Tabor, 1975; Snavely and Wagner, 1982a; Palmer and Lingley, 1989; Brandon and Calderwood, 1990; Orange and others, 1993). Poorly exposed thrust faults separate the lithic assemblages (Stewart, 1970; Lingley and others, 1996; Tabor and Cady, 1978b). Onshore, structures at all scales match those typically found in accretionary thrust belts. Directly offshore, reflection seismic profiles and interpretations (Snavely and Wagner, 1982b; McClellan and Snavely, 1987, 1988; Palmer and Lingley, 1989; Boyer and Lingley, 1991, 1994) clearly depict this thrust belt. The thrust faults are offset by younger, poorly exposed, high-angle strike-slip faults.

Three major structural sheets or domains have been identified in the Forks quadrangle, mainly on the basis of lithic assemblages (Figs. 4, 5). From the northeast, these are:

(1) The Huelsdonk sheet, which includes the Lake Ozette–Calawah Ridge block of Snavely and others (1993) and part of the Western Olympic lithic assemblage of Tabor and Cady (1978a);

(2) The Salmon River sheet, which includes part of Tabor and Cady's (1978a) Western Olympic lithic assemblage and

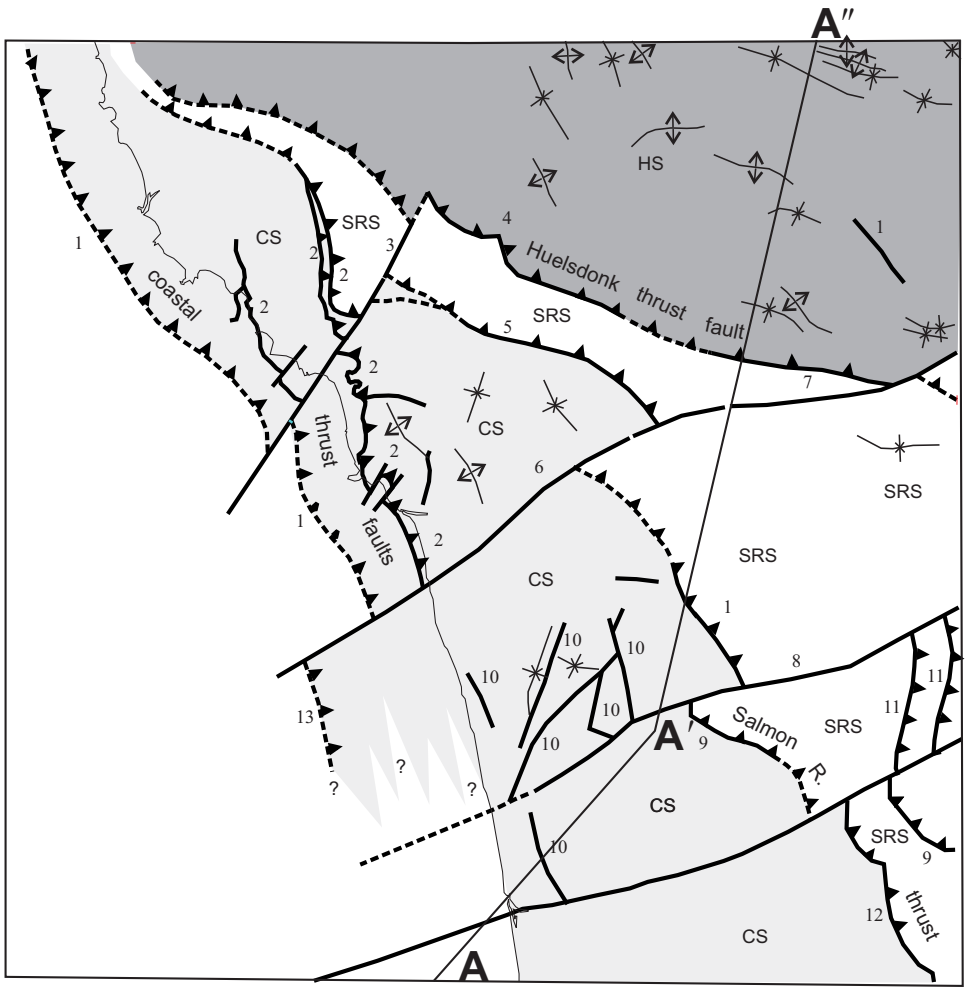

Figure 4. Major faults and folds in the Forks 1:100,000 quadrangle. The Huelsdonk (HS), Salmon River (SRS), and Coastal (CS) structural sheets have been mapped mainly using published and new dates, and also by connecting previously mapped fault segments into thrust systems. The fault connections are dashed where obscured or speculative. From the north, the fault segments are: (1) unnamed faults (Tabor and Cady, 1978a), (2) unnamed faults (Rau, 1979), (3) the Goodman Creek (left-lateral) strike-slip fault (Rau, 1979), (4) the Bogachiel fault (Rau, 1979), (5) the May Hill fault (Rau, 1979), and (6) the Hoh River fault (Rau, 1979), (7) the Huelsdonk, (8) Clearwater River, and (9) Salmon River shear zones of Stewart (1970), (10) unnamed faults (Rau, 1975), (11) unnamed faults, (12) an unnamed fault (Lingley and others, 1996), and (13) an extension of the coastal thrust system. The position and displacement of this extension is based on a probable piercing point along the Hoh River fault defined by zircon fission-track minimum ages on the Salmon River thrust fault. It is also based on the lack of mélange (unit ~~M~~Ebx) along the coast south of the Hoh River fault. Presumably, mélange is exposed offshore.

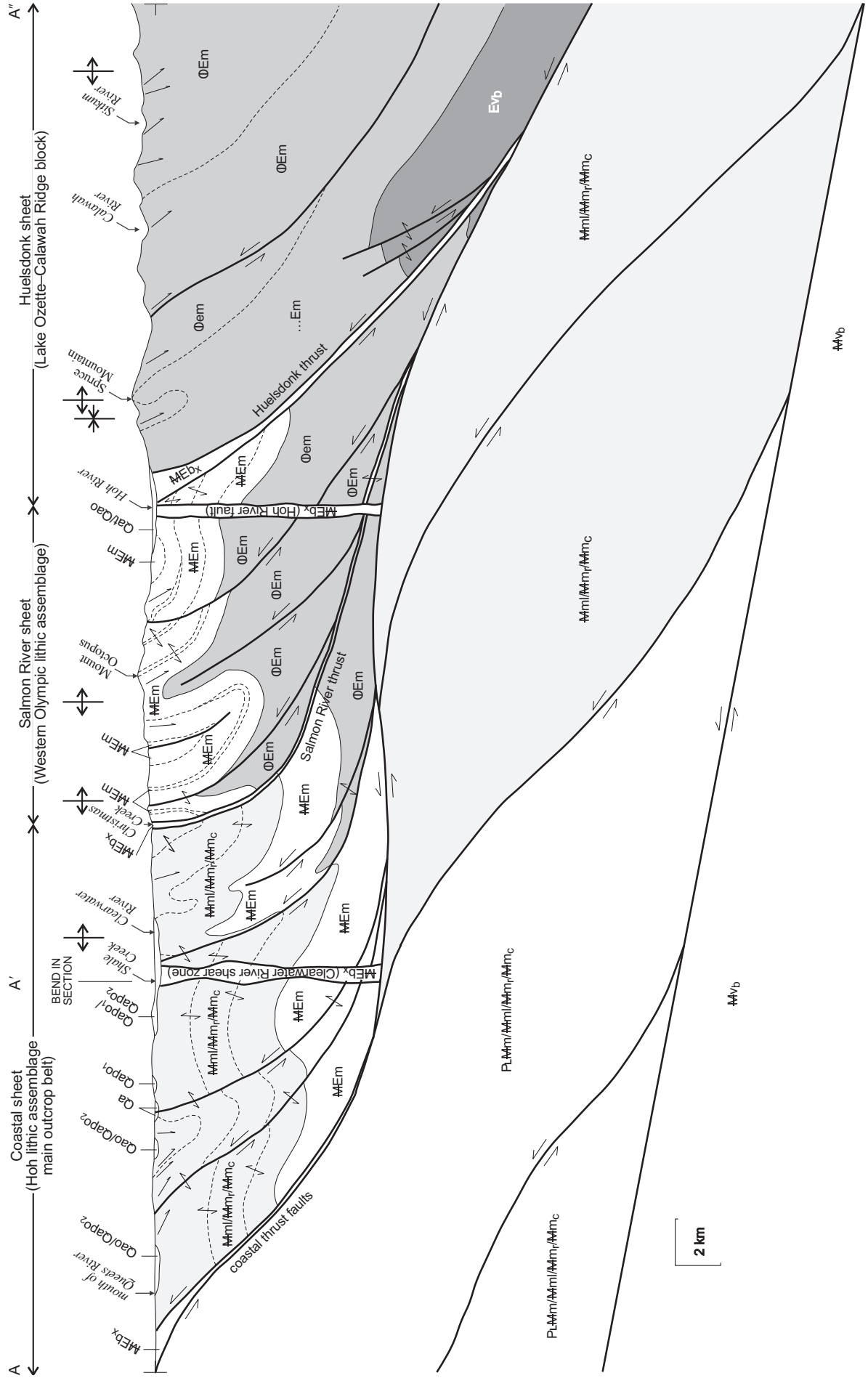

Figure 5. A schematic southwest-to-northeast structural cross section of the Forks 1:100,000 quadrangle showing the major structural sheets, probable thrust systems, and their possible relations to subsurface structure. The major features of this cross section are based on work by Palmer and Lingley (1989) and Boyer and Lingley (1991). The small-headed arrows are apparent dips along the line of section. Unit symbols (for example, MEm) are described in the text.

equivalent rocks in the Sams River–Matheny Creek area (Lingley and others, 1996); and

(3) The Coastal sheet, which includes the main outcrop belt of the Hoh lithic assemblage of Rau (1973).

These sheets appear to be hanging-wall sections of three major thrust faults—the Huelsdonk and Salmon River thrust faults of Stewart (1970) and an unnamed coastal thrust fault mapped by Tabor and Cady (1978a) and Rau (1979).[1]

Although the lithic assemblages are not mapped herein because the state mapping program (Schuster, 1994) is based on chronostratigraphy and because new dates allow somewhat improved stratigraphic resolution, the writers believe the lithic assemblages as originally mapped continue to have utility for understanding Olympic geology.

AGE DETERMINATIONS

Where possible, we have relied on paleontology (mostly Rau, 1975, 1979; Addicott, 1976) for determining the ages of mapped units. However, the bathyal sediments that dominate the stratigraphic sequence yield few diagnostic fauna, and most fossils have been lost to diagenesis east of the Salmon River thrust fault.

For this reason, we use zircon fission-track minimum ages to provide a guide to assist in segregating map units and resolving structure (Appendix, Plate 1), but not to control the interpretation. Fission tracks left as zircons decay can provide an estimate of the age of the youngest rocks eroded from the sediment provenance (Brandon and Vance, 1992). Interpretation of zircon fission tracks is a statistical process that is improved if the sample yields 50 or more zircon grains, but even these samples are subject to considerable uncertainty, typically ±5 Ma or more. The time needed to completely exhume and transport the sediment to the depositional site is not reflected in zircon fission-track minimum age dates.

These considerations not withstanding, zircon fission-track minimum ages in the western Olympic Peninsula have good agreement with paleontological interpretations from the same outcrops. In this study, we have relied on zircon fission-track minimum ages mainly to confirm contacts of the three major structural sheets.

DESCRIPTIONS OF MAP UNITS

The stratigraphic nomenclature used herein is summarized on Plate 2. The standard nomenclature used for the Washington State map project is described in Schuster (1994). The capital letters describe the applicable system or series, lowercase letters indicate the gross lithology, and subscripts refer to specific formations or detailed lithologies. For example, unit ~~M~~Eml$_c$ consists of Miocene to Eocene marine sedimentary rocks, which are dominantly lithic siliciclastic pebble conglomerates.

Quaternary Sedimentary Units

Qa **Alluvium (Pleistocene to Holocene)**—These deposits consist of stream sediments within active channels, including the approximate areas of the 100-year flood plains. In the Quinault, Queets, Hoh, upper and middle Bogachiel, and Calawah Rivers and their tributaries, unit Qa is composed of sediment derived from the Olympic Mountains. Within the Sol Duc, lower Bogachiel, and Quillayute channels, sediment sources include exotic rocks transported from the north by continental glaciers. West of the foothills, the alluvium also includes locally derived Miocene marine sedimentary and volcanic rocks. The low-gradient reaches of these rivers are characterized by large-amplitude, migrating meanders and large amounts of sediment input from adjacent landslides and debris flows.

Qls **Landslide deposits (Pleistocene to Holocene)**—Landslides include large rockfalls and deep-seated slump-earthflows that incorporate some combination of soil, talus, colluvium, bedrock, and fluvial and glacial sediments. Unit Qls includes both landslide deposits and associated landslide headscarps. Landslide deposits are typically chaotic and poorly sorted, consisting of material derived from older geologic units. Landslides occur throughout the map area in drainage headwalls, on lower slopes, at the bases of slopes, and along terrace edges. Their relative ages are inferred from stratigraphic position, age of parent materials, and geomorphic expression. Many deep-seated landslides occur along the coast in tectonic mélange or breccia (unit ~~M~~Ebx).

Landslides are common on the Olympic Peninsula because of weak geologic materials, steep topography, and high annual precipitation. Landslides in bedrock commonly occur along bedding surfaces, within shear and mineralogically altered zones, and along structural weaknesses within rock units. Landslides are also common where dense, fine-grained sediments (such as till or lacustrine deposits) within valley-fill sequences create barriers to ground-water flow. The terrace-edge landslides are some of the largest in area (Gerstel, 1999) and provide chronic input of fine sediment into river channels.

In conjunction with this mapping project, an inventory of deep-seated landslides was compiled for the Forks quadrangle and one additional 7.5-minute quadrangle to the northeast (Slide Peak) (Gerstel, 1999). Inventoried landslides were classified based on a five-category 'level of certainty' rating system, with level 1 indicating the highest level of confidence in landslide identification. To avoid obscuring the bedrock and glacially derived surficial deposits that are the focus of this geologic map compilation, we chose not to show all inventoried landslides here; instead, only landslides rated with certainty levels 1 and 2 are shown.

Qao **Alpine glacial outwash (late Wisconsinan; Fraser age)**—These youngest of the alpine outwash deposits are generally unconsolidated to weakly consolidated, weakly (where deposition was ice-proximal) to well-stratified sequences of cobble and pebble gravel in a tan to buff sandy matrix. Clast size is variable, dominated by 10 to 20 cm cobbles with occasional boulders greater than 1 m in diameter. In some areas, the outwash is capped by up to 0.5 m of massive light tan to buff silt and clayey silt (loess). The outwash deposits discontinuously cap coastal bluffs between Abbey Island and Steamboat Creek, and are exposed in most

[1] The offshore fault controlling this sheet has been interpreted as west-dipping by Snavely and Kvenvolden (1989), but we favor Tabor and Cady's original east-dipping interpretation (1978b). See the discussion in Structure below.

valley bottoms of the larger rivers. In the valleys, they form the upper 3–10 m of the terraces within 10–30 m in elevation above the alluvium (unit Qa). The outwash is derived solely from Olympic Peninsula rocks, which distinguishes these deposits from those left by the Juan de Fuca lobe of the continental glacier. Upvalley limits of outwash deposits are commonly defined by moraines of similar age.

During Fraser time, the Hoh valley glacier margin occupied a position at the head of the Snahapish valley, possibly spilling a small amount of outwash into the upper Snahapish valley, but not extending downstream to the Clearwater River, as it did during pre-Fraser glacial advances (Thackray, 1996; Wegmann, 1999).

Fraser-age alpine outwash deposits include several advances of the Hoh Oxbow drift of Thackray (1996), ranging in age from about 39,000 to 19,500 yr B.P. Also included in this unit are deposits of the Twin Creeks drift of Thackray (1996), best exposed at the confluence of the main and south forks of the Hoh River. Fraser-age deposits are correlated to oxygen-isotope stage 2.

Qat **Alpine glacial till (late Wisconsinan; Fraser age and younger?)**—Generally exposed as lodgment till, these deposits are dense, very compact, and poorly sorted, containing rounded to subrounded to subangular clasts in a gray to tan clay-silt matrix. Clasts are derived solely from Olympic Peninsula rocks. Deposits range from stratified to unstratified. They may be weakly oxidized to depths of 1 m. The dense nature of the deposits results in low permeability, often causing saturation of the overlying sediment or soil and consequent landsliding.

Locally, unit Qat may occur as moraines and ablation till. Where deposits mapped as Qat occur as moraines, they consist of unconsolidated diamicton with lenses of stratified sand, gravel, silt, or clay. Moraines are generally arcuate in shape and lie within valley bottoms. Some Qat moraines in cirques of the Olympic Mountains may be Holocene in age. Ablation till is mapped in the Hoh valley north and south of the Highway 101 crossing, upstream of the Hoh oxbow.

Fraser-age till was deposited by the least extensive of the alpine glacial advances recognized on the west side of the Olympic Peninsula. In the Bogachiel River valley, radiocarbon dates indicate that Fraser-age glaciers did not extend westward beyond the Olympic National Park boundary. In the Hoh and Queets valleys, radiocarbon ages indicate Fraser-age ice extended to about 45 and 32 km beyond the range front, respectively.

Unit Qat includes deposits of several advances of the Hoh Oxbow glaciation of Thackray (1996), ranging in age from about 39,000 to 20,000 yr B.P. It also incorporates deposits of the Twin Creeks advance of Thackray (1996), assigned an age of ~19,000–17,000 yr B.P., and an undated later readvance. The deposits of the readvance are best exposed at the confluence of the main and south forks of the Hoh River.

Qad **Alpine glacial drift (late Wisconsinan; Fraser age)**—Deposits mapped as unit Qad may include outwash, till, and lacustrine sediments. Ablation till and deposits underlying dead-ice topography are also mapped as Qad. Drift is mapped where several depositional environments are represented by deposits in near-vertical exposures, as along stream banks. Unit Qad underlies much of the valley bottom adjacent to the Hoh River, upstream of the Hoh oxbow.

Unit Qad deposits are equivalent in age to moraines of the Hoh Oxbow glaciation mapped by Thackray (1996).

Qapo **Alpine glacial outwash (early to mid-Wisconsinan age)**—This is the youngest of the three pre-Fraser drift units. The deposits are similar to unit Qao in grain-size distribution, clast lithology, and bedding characteristics, but are weathered to 1–2 m deep and are commonly capped by mottled tan-gray to pale orange silt and clayey silt (loess). The loess is commonly bioturbated, incorporating cobbles from the underlying outwash. Unit Qapo deposits are generally weakly consolidated and consist of cobbles and gravel in a sandy matrix. Clasts are dominantly 10–20 cm in size, with occasional boulders larger than 1 m. The clast-to-matrix ratio is variable.

Unit Qapo deposits are found in most of the larger valleys; they form the upper 3–10 m of terraces, with surfaces 30–60 m above the active channels. They are also exposed near the surface in coastal bluffs 5–7 km to the north and south of the Queets River, a few kilometers south of the Hoh River, and underlying unit Qao deposits south of Destruction Island viewpoint. Clasts are derived solely from Olympic Peninsula rocks. Outwash from the younger pre-Fraser glaciers in the Hoh valley was deposited into the Snahapish and Clearwater drainages and into the Bogachiel valley north of the divide with the Hoh valley. Here the Hoh glacier bifurcated, with one branch flowing northward ~1.5 km from the Hoh valley into the Bogachiel valley.

These younger pre-Fraser outwash deposits are equivalent in age to the early or middle Wisconsinan Lyman Rapids drift of Thackray (1996). They probably correlate to oxygen-isotope stage 4 or 3, but might be as old as stage 5b. Minimum-age radiocarbon dating and stratigraphic correlations suggest an age of ~55,000–110,000 yr B.P. (Thackray, 1996). It should be noted that in some drainages there may be very little difference in age between this drift and the Fraser-age drift.

Qapt **Alpine glacial till (early to mid-Wisconsinan age)**—These deposits generally occur as lodgment till, characteristically unstratified compact deposits of rounded to subrounded to subangular clasts in a clay and silt matrix. Clasts are derived solely from Olympic Peninsula rocks. Where till forms moraines, the deposits are commonly less consolidated than lodgement till and weakly bedded. In places, the till is capped by up to 2 m of loess where outwash either was not deposited or was removed by subsequent glacial erosion. Where unit Qapt occurs as lodgment till, the overlying loess incorporates few cobbles from the till, because bioturbation is usually limited to the loess in those locations.

Unit Qapt moraines are broad and of relatively low relief. They form long, nested, lobate ridges in the

lower Queets valley; in the Hoh valley, terminal moraines bifurcated near the present divide between the Hoh and Bogachiel basins. Unit Qapt moraines are not apparent in the Bogachiel drainage, possibly due to burial by subsequent alpine or continental outwash. Unit Qapt is also found as ablation till, which can be seen along the Queets River upstream of its confluence with the Clearwater River and inboard of Thackray's (1996) Lyman Rapids terminal moraine a few miles downstream of the confluence with the Salmon River.

Unit Qapt deposits are equivalent in age to drift of the Lyman Rapids advance of Thackray (1996), suggesting a minimum age of ~55,000 yr B.P.

Qap **Undifferentiated alpine glacial drift (early to mid-Wisconsinan age)**—Deposits mapped as unit Qap may include outwash, till, and lacustrine sediments. Ablation till and deposits underlying dead-ice topography are mapped as unit Qap. Drift is also mapped where several depositional environments are represented in near-vertical exposures, as along stream banks. Unit Qap underlies much of the valley bottom adjacent to the Sitkum River, as well as a small area along the Salmon River.

$Qapwo_2$ **Alpine glacial outwash (younger pre-Wisconsinan age)**—Deposits are generally composed of clast-supported cobbles and gravel in a clayey sand and silt matrix. They are characterized by orange and white weathering and alteration to more than 4 m depth, with punky clasts of Olympic Peninsula materials. In the northern map area, these deposits include scattered clasts of reworked older continental deposits, identified by clasts derived from the North Cascades or British Columbia. In the lower Queets and Hoh valleys, deposits lie outboard of unit $Qapwt_2$ moraines and dominate the lowland along the southern boundary of the quadrangle, forming terrace surfaces at about 125 m elevation. On the south side of the Quillayute River, unit $Qapwo_2$ is included in deposits mapped as drift (unit $Qapw_2$) where outwash deposits are too small to map at this scale. They are also included as unit $Qapw_2$ where incision by the river exposes a sequence of (from bottom to top) bedrock, advance outwash, till, recessional outwash, and loess.

Unit $Qapwo_2$ includes primarily outwash of the Whale Creek advance of Thackray (1996) and may be Illinoian in age (late pre-Wisconsinan), possibly as old as 200,000 yr B.P. Unit $Qapwo_2$ may also include some Wolf Creek–age outwash.

$Qapwt_2$, $Qapwt_{2m}$ **Alpine glacial till (younger pre-Wisconsinan)**—Deposits are gravel, cobbles, and boulders supported in a very dense clay and silt matrix, characterized by orange-colored weathering, commonly to more than 4 m depth. Clasts are derived predominantly from Olympic Peninsula rocks, but include some clasts of reworked older Juan de Fuca lobe glacial deposits. Clasts generally range in size from 3 to 30 cm. Till thickness ranges from a thin veneer to at least 3 m in the Goodman and Murphy Creek drainages. Unit $Qapwt_2$ is commonly overlain by outwash (unit $Qapwo_2$) and capped by 2–3 m of loess, as on the south side of the Quillayute River and in the Goodman Creek drainage.

No moraines are preserved from this advance in the northern part of the quadrangle, probably due to burial or erosion by subsequent alpine and continental glaciations. Prominent nested moraines (unit $Qapwt_{2m}$ on Plate 1 and in GIS database) with crest elevations of about 344 m above sea level are located on both sides of the Queets valley. The moraine crests are traceable from near the confluence with the Salmon River to a terminal position about 15 km downstream, where they are breached by the Queets River. Moraine morphology is very subdued, but the moraines rise slightly above the outwash plain into which they grade at about 125 m above sea level. No distinct $Qapwt_2$ moraines can be seen in the Hoh or Quillayute valleys, except possibly on the south side of Anderson Ridge (Tabor and Cady, 1978a).

Unit $Qapwt_2$ represents till of the Whale Creek advance of Thackray (1996) and may be Illinoian in age (late pre-Wisconsinan), possibly around 200,000 yr B.P.

$Qapw_2$ **Undifferentiated alpine glacial drift (younger pre-Wisconsinan age)**—Deposits mapped as unit $Qapw_2$ include outwash, till, and lacustrine sediments, which are mapped together when they cannot confidently be assigned to any particular depositional environment or when several depositional environments are represented in near-vertical exposures, as along stream banks. Although unit $Qapw_2$ is mostly till, the area adjacent to the Quillayute River and within the Goodman Creek drainage is mapped as drift for the above reasons. Ablation till and deposits underlying dead-ice topography are also mapped as unit $Qapw_2$. Up to 4 m of cobbly outwash deposits of this younger pre-Wisconsinan drift are exposed in coastal bluffs overlying unit ~~M~~Ebx for several miles south of the Quillayute River. Unit $Qapw_2$ is also mapped where exposures of either till (unit $Qapwt_2$) or outwash (unit $Qapwo_2$) are too small to map.

Glaciolacustrine deposits are not mapped as a separate unit because they are usually found in near-vertical river bank exposures or described in well logs where they are overlain by other sediments. Lacustrine sediments are commonly involved in large-scale deep-seated landsliding. They have also been important in reconstructing the depositional environments and history of ice advances and retreats, occasionally yielding organic material for radiocarbon dating. Lacustrine deposits in the Hoh and Queets valleys suggest that lakes commonly formed behind terminal moraines during alpine-ice recessional periods. However, well logs from west of Forks on Quillayute Prairie suggest extensive lacustrine deposits at depths greater than 30 m. These may be related to continental glaciation of Fraser age.

Deposits mapped as unit $Qapw_2$ include primarily drift of the Whale Creek advance of Thackray (1996) and may be Illinoian in age (late pre-Wisconsinan), possibly around 200,000 yr B.P.

$Qapwo_1$ **Alpine glacial outwash (older pre-Wisconsinan age)**—Deposits of unit $Qapwo_1$ are similar in character to deposits of unit $Qapwo_2$. In the Forks quadran-

gle, unit $Qapwo_1$ is mapped only in the Queets drainage over a small area outboard of the right lateral unit $Qapwt_1$ moraine. Unit $Qapwo_1$ deposits also crop out to the south in the Copalis Beach 1:100,000 quadrangle (Logan, in progress).

Unit $Qapwo_1$ corresponds to the Wolf Creek drift of Thackray (1996). Stratigraphic correlations with reversely magnetized lacustrine sediments suggest a minimum age of 780,000 yr B.P.

$Qapwt_1$, $Qapwt_{1m}$ **Alpine glacial till (older pre-Wisconsinan age)**—Similar in character to deposits of unit $Qapwt_2$, this unit is mapped only in the Queets drainage. Unit $Qapwt_1$ occurs as a subdued morainal ridge (labeled as unit $Qapwt_{1m}$ on Plate 1 and in GIS database) adjacent to and outboard of the unit $Qapwt_2$ moraine on the north side of the valley. The complementary left lateral moraine occurs in the Copalis Beach 1:100,000 quadrangle to the south (Logan, in progress), although a small remnant of the upvalley segment is mapped in the Queets valley between Matheny Creek and the Salmon River.

Unit $Qapwt_1$ corresponds to the Wolf Creek drift of Thackray (1996). Stratigraphic correlations with reversely magnetized lacustrine sediments suggest a minimum age of 780,000 yr B.P.

Qgo **Continental glacial outwash, recessional (late Wisconsinan; Fraser age)**—This unit was deposited by the Juan de Fuca lobe of the Cordilleran ice sheet and is characterized by unconsolidated, well-stratified cobbles in a loose gravelly sand matrix, with abundant boulders exceeding 1 m in diameter. Unit Qgo deposits include areas of bedded and reworked outwash that may be part of the active alluvium in the Sol Duc, North Fork Calawah, lower Bogachiel, and Quillayute valleys. The coarse nature of these deposits makes them highly permeable and well-drained. Unit Qgo deposits are found mostly north of Forks and the Quillayute River and form at least three major terrace surfaces between about 31 m and 63 m above sea level in the Sol Duc and Quillayute River valleys. Unit Qgo deposits probably exceed 50 m in thickness in places.

About 60 percent of the clasts are locally derived Olympic Peninsula rocks and about 40 percent are derived from distal sources, including granitic and metamorphic rocks from the North Cascades and British Columbia. The presence of granite is used as an indicator of deposition by the Juan de Fuca lobe of the continental ice sheet. Well logs from the Forks area suggest that much of the area covered by unit Qgo is underlain by lacustrine deposits, particularly under Quillayute Prairie.

Unit Qgo is associated with the Vashon Stade of the Fraser Glaciation. A radiocarbon sample from outwash deposits exposed in a bank of the Sol Duc River about 2 km north of Forks yielded a date of about 12,500 yr B.P. (Table 1, Beta #116786). The sample was collected from the base of the outwash near its contact with the underlying till, suggesting that recession had not been in progress long. Drift from alpine glaciers underlies unit Qgo deposits in the Sol Duc valley, suggesting that the alpine glaciers had reached their maximum and retreated upvalley earlier than the arrival of continental ice.

Qgt **Continental glacial till (late Wisconsinan; Fraser age)**—Unit Qgt deposits of the Juan de Fuca lobe of the Cordilleran ice sheet are dense to extremely dense diamicton with cobbles, gravel, and scattered boulders supported by a clay and silt matrix. Unit Qgt deposits are usually gray to brown in color and are commonly weakly oxidized to <1 m depth where not overlain by recessional outwash; the weathering profile may be shallower to nonexistent where till is overlain by outwash. Unit Qgt deposits range in thickness from <1 m to about 4 m. Clasts are derived from local Olympic Peninsula rocks as well as materials trans-

Table 1. Age data collected during this compilation. See Appendix 1 for the data from the zircon fission-track analyses and references in the text for data in other published studies

Map location no.	Sample no.	Unit	Age	Type
1	WSL 7-98-5 (195)	~~M~~ml	25.8 ±3.0 my	zircon fission track
2	Stewart 91-72 (143)	~~M~~Eml	22.1 ±0.8 my	zircon fission track
3	Stewart 94-15 (171)	~~M~~Em$_r$	21.6 ±1.6 my	zircon fission track
4	WSL 10-93-6	~~M~~Em$_r$	Narizian (middle to upper Eocene)	foraminifera
5	Stewart 93-4 (152)	~~M~~Eml	37.5 ±8.4 my	zircon fission track
6	Stewart 93-49 (178)	~~M~~Eml	32.3 ±4.3 my	zircon fission track
7	Stewart 95-13 (170)	~~M~~Em$_r$	24.4 ±1.3 my	zircon fission track
8	Stewart 93-22 (154)	~~M~~Em	21.0 ±0.9 my	zircon fission track
9	Stewart 95-11 (169)	OEm	33.0 ±3.7 my	zircon fission track
10	Hoh-1 (128)	OEm	47.2 ±2.5 my	zircon fission track
11	WG72998-2a (Beta #21533)	$Qapwt_2$	> 43,980 yr B.P.	radiocarbon
12	Bog-1 (94)	~~M~~Em (~~M~~Ebx?)	32.4 ±4.2 my	zircon fission track
13	WG72998-3 (Beta #123942)	$Qapw_2$	> 47,000 yr B.P.	radiocarbon
14	WG72998-4 (Beta #121534)	$Qapwt_2$	> 47,400 yr B.P.	radiocarbon
15	Stewart 94-42 (167)	OEm	40.2 ±3.7 my	zircon fission track
16	Stewart 94-41 (189)	OEm	39.2 ±2.2 my	zircon fission track
17	WG9397-2a (Beta #116786)	Qgo	12,570 ±6 yr B.P.	radiocarbon
18	Stewart 94-40 (166)	OEm	44.6 ±5.3 my	zircon fission track
19	Arc 88-12 (34)	OEm	54.6 ±2.4 my	zircon fission track

ported from regions to the north and northeast. The presence of granites and metamorphics is an indication of deposition by the Juan de Fuca lobe of the continental ice sheet. Exposures of this unit are limited to the northwest portion of the Forks quadrangle, north of the Sol Duc and Quillayute Rivers.

The Juan de Fuca lobe of the continental ice sheet occupied the Strait of Juan de Fuca and covered the northern edge of the Olympic Peninsula from at least 15,000 yr B.P. (Heusser, 1973b; Schasse, in progress) to about 13,000 yr B.P. (Gerstel, 1997; this report). A radiocarbon date on wood from till in the Dickey Creek drainage yielded an age of about 13,200 (Beta # 123219; Schasse, in progress). Wood in outwash (unit Qgo) exposed along the Sol Duc River yielded a date of about 12,500 yr B.P. (Table 1, Beta #116786), suggesting that ice had retreated from the Forks area by then.

Qgd **Undifferentiated continental glacial drift (late Wisconsinan; Fraser age)**—Deposits left by the Juan de Fuca lobe of the continental glacier are mapped as undifferentiated drift where a combination of depositional environments is represented or no characteristic sediment type is dominant. These deposits can include outwash, till, and lacustrine sediments and are predominantly of Vashon age, although some may correlate to pre-Vashon glaciations.

Qgdc **Glacial and nonglacial deposits (Fraser age or older)**—These deposits consist of stratified fluvial cobbles and gravel exposed in sea cliffs of the marine terraces near Kalaloch Creek. Unit Qgdc deposits are generally oxidized to 1–3 m and capped with 1–2 m of loess. They are probably reworked from units Qapo and $Qapwo_2$ and alluvium from Kalaloch Creek. Deposits are gently dipping and laterally continuous, suggesting deposition in a beach environment and reworking by coastal waves. Some cut-and-fill structures and foreset beds exist.

Tertiary Lithologic Units

SEDIMENTARY ROCKS

PMm **Marine sandstone, siltstone, and conglomerate (Pliocene to Upper Miocene)**—Unit PMm consists of medium- to coarse-grained sandstones with lenses of fossiliferous conglomerate and sandy fossiliferous siltstone. It is restricted to a few small outcrops on the coastal sheet, but offshore, a minimum of several hundred meters of section are present (Palmer and Lingley, 1989).

Unit PMm includes the Quillayute Formation of Reagan (1909), unit Tqy of Rau (1979), and unit Tqq of Tabor and Cady (1978a).

The age of unit PMm is Pliocene to Late Miocene. (See discussion in Rau, 1979.) It unconformably overlies unit Mmr and is unconformably overlain by units Qao and Qa. Rocks of unit PMm are interpreted as shallow marine deposits (Rau, 1979; Stewart, 1970).

Mml_c **Marine pebble conglomerate (Lower to Middle Miocene)**—Unit Mml_c consists of clast-supported pebble conglomerate with well-rounded, ellipsoidal to subspherical pebbles and conglomeratic sandstone.

Beds are mostly 0.5–4 m thick and generally discontinuous along strike. Individual beds show little internal structure, but weak imbrication has been observed locally.

Pebbles include siliciclastic rocks of probable local origin together with chert, volcanic rocks, and minor granitoid, limestone, and quartzite clasts. Within each bed, lithic sandstone clasts display variable induration. Typically, pebbles range from 0.5–3 cm. Unit Mml_c does not include the granule and rip-up clast conglomerates or breccia, which are mapped as part of unit Mml. Unit Mml_c varies from gray, brownish gray, and greenish gray to very dark gray. Weathering colors are generally medium to dark gray.

Unit Mml_c includes unit Thcs of Rau (1975, 1979), parts of units Thsu and Thc of Lingley and others (1996), and units Twoc and Thc of Tabor and Cady (1978a). These rocks are included in Lithofacies III of Lingley (1995).

The age of unit Mml_c is Early to Middle Miocene (Rau 1975, 1979). It generally has conformable relations with coeval units Mml and Mm_r.

Rocks of unit Mml_c are interpreted as channel facies deposited from debris flows in a bathyal open-marine environment (Lingley, 1995; Rau, 1979; Stewart, 1970).

Mm_r **Marine rhythmic thin- to medium-bedded sandstone and shale or slate (lower to middle Miocene)**—Unit Mm_r is a monotonous sequence of gray, very fine- to medium-grained, feldspatholithic to lithofeldspathic sandstones and very dark gray siltstone and shale or slate, much of which is rhythmically bedded (Rau, 1979; Tabor and Cady, 1978a; Weissenborn and Snavely, 1968). The sandstone to siltstone plus slate ratio is generally greater than 1.

Bedding characteristics are most useful for identifying this unit. With rare exceptions, bed thickness ranges from laminations to less than 50 cm and averages about 10 cm. Most of these rocks are parallel bedded with little or no variation in thickness observed at outcrop scale. Basal and upper contacts are generally sharp, but a few sequences are composed of a basal sandstone bed that grades upward into laminated siltstone and (or) shale. Most individual sandstone beds are laminated.

Unit Mm_r varies from gray, brownish gray, or olive gray to very dark gray. Sandstone beds and laminations are lighter colored. Detrital muscovite and very dark gray, platy rip-up clasts are common in the sandstones. The sandstone and siltstone beds have blocky weathering profiles and commonly form a colluvium of 2 x 2 x 4-cm blocks. Weathering colors are generally medium to dark gray, yellowish red (5YR5/8 to 7.5YR5/8) (Munsell Color Corp., 1975), medium reddish brown, or a distinctive reddish yellow (7.5YR6/8).

Unit Mm_r includes units Thsl, Thlm, and Thss of Rau (1975, 1979) and Lingley and others (1996) and units Thr, Thsr, and Twor of Tabor and Cady (1978a). These rocks are included in Lithofacies I and IV of Lingley (1995).

In the western portion of the map area, the age of unit Mm_r is well constrained as Early to Middle Mio-

cene (25–14 Ma) by numerous microfossil and macrofossil determinations (Addicott, 1976; Rau, 1975, 1979), stratigraphic position (Palmer and Lingley, 1989), and zircon fission-track ages. In the eastern part of the map area, the age is poorly constrained as Early Miocene by zircon fission-track minimum ages. This unit generally shows conformable relations with coeval units Mml and Mml_c. It is inferred to be in fault contact with units MEm and OEm.

Rocks of unit Mm_r are interpreted as submarine interchannel and levee facies deposited in middle to lower bathyal open-marine environments (Stewart, 1970; Rau, 1979; Lingley, 1995).

Mml **Marine clastic rocks, dominantly thick-bedded lithic sandstone (Lower to Middle Miocene)**—Unit Mml is composed mainly of nongraded, 1–50 m thick, multistory lithic sandstones and matrix-supported granule conglomerates. These coarse-grained rocks are laterally discontinuous and vertically separated by a few meters to more than 100 m of thin- to medium-bedded shales and laminated siltstones similar to those of unit Mm_r.

Most unit Mml exposures include five or more vertically stacked beds, ranging from 0.5 to 5 m thick. Except for rare poorly developed, normally graded beds, most sandstone beds are massive. However, individual thick sandstone beds with massive bases and widely spaced, parallel laminations and (or) parallel banding developed within a meter of the top are also present. Both the massive sandstone sequences and sandstone beds with laminated/banded tops are generally lenticular on an outcrop scale, although map patterns suggest that some larger packets are tabular. Dish structures are present in some outcrops, and loading features are present on some bedding planes. Rare tool marks and current lineations generally trend northeast or southwest. A few Bouma sequences have been observed in the Kalaloch Creek basin.

The sandstone and granule conglomerates are lithic to lithofeldspathic arenites (Dickinson, 1970). They are medium- to very coarse-grained and moderately to well-sorted. Most massive or laminated/banded sandstone beds contain rip-up clasts or intraclasts of mudstone, very dark-gray siltstone, and (or) tuffaceous siltstone. These clasts are generally tabular, range from 0.3 mm to more than 30 cm in length, and are oriented parallel to bedding. Many of the tabular rip-up clasts taper to very thin, fragile edges. They are gray, dark gray, or olive gray and weather tan or light gray.

Unit Mml includes unit Ths of Rau (1975, 1979), unit Thts of Lingley and others (1996) and units Thts and Thsp of Tabor and Cady (1978a). These rocks are included in Lithofacies II and III of Lingley (1995).

As in unit Mm_r, the age of unit Mml is constrained as Early to Middle Miocene (25–14 Ma) in the Coastal structural sheet (Rau 1975, 1979), but poorly constrained by zircon fission-track minimum ages in the Salmon River structural sheet (Plate 1). Unit Mml generally shows conformable relations with units Mm_r and Mml_c. It is inferred to be in fault contact with unit OEm.

The massive to thick-bedded sandstones in unit Mml were mostly deposited from sandy debris flows in a bathyal open-marine environment (Lingley, 1995). Thin-bedded rocks within unit Mml are mostly interpreted as deep-marine interdistributary and levee deposits.

MEm **Marine sedimentary rocks, undivided (Miocene to Eocene)**—Unit MEm consists of undivided thick- and thin-bedded sandstone and conglomerate and thin-bedded siltstone, shale, or slate. It includes rocks with lithologies and sedimentary structures similar to those of units MEml, MEm_r, and $MEml_c$ that have not been mapped in sufficient detail to subdivide at 1:100,000 scale. Also included are rocks with no age control.

Unit MEm includes unit Tur of Tabor and Cady (1978a) and unit Thsu of Lingley and others (1996).

An Early Miocene to Middle Eocene age (14–48 Ma) is assigned to unit MEm on the basis of a limited number of zircon fission-track minimum ages (Plate 1) and one sample containing a Narizian faunal assemblage (Lingley, 1995). Unit MEm is inferred to be in fault contact with units Mm_r and MEml. The dearth of detailed mapping precludes facies identification.

MEm_r **Marine rhythmic thin- to medium-bedded sandstone, siltstone, and shale or slate (Miocene to Eocene)**—Unit MEm_r consists of thin-bedded, very fine-grained sandstone, siltstone, and shale in the western part of the quadrangle or slate in the eastern part (Tabor and Cady, 1978a). These rocks are similar to those of unit Mm_r.

Although thin, discontinuous, relict beds and laminations of very fine-grained sandstone and siltstone are present, most bedding has been stretched and rotated to the point where only phacoids remain. Unit MEm_r varies in color from very dark gray to black and weathers mostly gray to brown.

Unit MEm_r includes units Thsr, Twos, and Two of Tabor and Cady (1978a) where these occur south of the Hoh River. It also includes their unit Thsr in the headwaters of the Snahapish and Clearwater Rivers. These rocks are included in Lithofacies I and IV of Lingley (1995).

The age of unit MEm_r is mostly Early Miocene as determined by fossil assemblages (Tabor and Cady, 1978a) and zircon fission-track minimum ages (Plate 1). However, a few Narizian and Zemorrian foraminifera have been recovered (Tabor and Cady, 1978a; Lingley, 1995) and four Late Eocene to Middle Oligocene fission-track minimum ages have been recorded. (See Plate 1). This broad age range probably results from tectonic intercalation along unmapped thrust faults. Unit MEm_r is interpreted as having conformable relations with coeval units MEml and $MEml_c$. Rocks of unit MEm_r are interpreted as deep-marine facies similar to those of unit Mm_r (Lingley, 1995; Rau, 1979; Stewart, 1970).

MEml **Marine clastic rocks, dominantly thick-bedded lithic sandstone (Miocene to Eocene)**—Unit MEml closely resembles unit Mml and is composed mainly of massive sandstones and matrix-supported granule conglomerates in laterally discontinuous multistory packets up to 40 m in thickness. The coarse-grained

packets are separated by tens to hundreds of meters of thin- to medium-bedded slates and laminated siltstones similar to unit ~~M~~Em$_r$.

The sandstones are medium- to very coarse-grained and moderately to well-sorted. As in unit ~~M~~ml, rip-up clasts or intraclasts of mudstone, very dark-gray siltstone, and (or) tuffaceous siltstone are the most important accessory. These intraclasts are dark gray, gray, or greenish gray, weather tan, and are typically angular with fragile edges.

Unit ~~M~~Eml includes Tabor and Cady's (1978a) units Thts and Thc, part of unit Tur in the headwaters of the Snahapish and Clearwater Rivers, and part of units Twoc and Twot between the headwaters of the Clearwater River and South Fork Hoh River. It is also equivalent to unit Thts of Lingley and others (1996) south of the Queets River. These rocks are included in Lithofacies II of Lingley (1995).

The minimum age of unit ~~M~~Eml is poorly constrained by a few zircon fission-track ages that range from Early Miocene to Middle Eocene (Plate 1). Unit ~~M~~Eml generally shows conformable relations with unit ~~M~~Em$_r$, but is in probable fault contact with unit OEm and the Miocene rocks described above.

The massive to thick-bedded sandstones in unit ~~M~~Eml were mostly deposited from sandy debris flows in a bathyal open-marine environment (Lingley, 1995). Thin-bedded rocks within this sequence are mostly interpreted as deep-marine interchannel and levee deposits.

~~M~~Eml$_c$ **Marine pebble conglomerate (Lower Miocene to Eocene)**—Unit ~~M~~Eml$_c$ consists of well-rounded, ellipsoid to subspherical clast-supported pebble conglomerate and conglomeratic sandstone, which are lithologically indistinguishable from unit ~~M~~ml$_c$ with available data.

Unit ~~M~~Eml$_c$ varies in color from gray, olive gray, and greenish gray to very dark gray and commonly contains dark greenish gray (GLEY4/1–GLEY3/1) altered volcanogenic clasts. Weathering colors are generally medium to dark gray or dark greenish gray.

Unit ~~M~~Eml$_c$ includes parts of units Twoc and Thc of Tabor and Cady (1978a). These rocks are included in Lithofacies III of Lingley (1995).

Unit ~~M~~Eml$_c$ has conformable relations with coeval units ~~M~~Eml and ~~M~~Em$_r$. The age of unit ~~M~~Eml$_c$ is poorly constrained by zircon fission-track minimum dates from adjacent, conformable units as Middle Miocene to Middle Eocene. Rocks of ~~M~~Eml$_c$ are interpreted as channel facies deposited from debris flows in a bathyal open-marine environment (Lingley, 1995).

OEm, OEm$_o$ **Marine sedimentary rocks, undivided, and marine sedimentary rocks of the Ozette Lake–Calawah Ridge block (Oligocene to Eocene)**—Units OEm and OEm$_o$ consist of sandstone, both thick- and thin-bedded, and thinly bedded siltstone, shale, and slate with traces of coal. Locally these include granule conglomerates. These units contain rocks whose lithologies and sedimentary structures are similar to those of units ~~M~~m$_r$, ~~M~~ml, ~~M~~Eml, and ~~M~~Em$_r$, but the rocks of units OEm and OEm$_o$ have not been mapped with sufficient detail in the Forks quadrangle to subdivide at 1:100,000 scale.

Outcrops in the northwestern corner of the Forks 1:100,000 quadrangle are contiguous with rocks included in the Lake Ozette–Calawah Ridge block of Snavely and others (1993). Schasse (in progress) designated these rocks as unit OEm$_o$ on the Cape Flattery 1:100,000 quadrangle. Tabor and Cady (1978a) mapped these rocks together with undifferentiated strata farther east as part of their Western Olympic lithic assemblage. Therefore, we map these strata as unit OEm$_o$ west of the fault that forms the Sol Duc River valley (Snavely and others, 1993) and as unit OEm farther east.

The ages of units OEm and OEm$_o$ are moderately constrained by several Narizian foraminiferal assemblages (Tabor and Cady, 1978a; Snavely and others, 1993) and numerous Early Eocene to Late Oligocene zircon fission-track minimum ages (Plate 1). Units OEm and OEm$_o$ are inferred to be in fault contact with ~~M~~Em$_r$ and ~~M~~Eml along the upper Hoh River. Rocks of units OEm and OEm$_o$ are interpreted as deep-marine deposits (Snavely and others, 1993).

OEml$_c$ **Marine pebble conglomerate (Oligocene to Eocene)**—Unit OEml$_c$, as described by Snavely and others (1993), consists of lithic sandstone and siltstone and mudflow conglomerate. Clast-supported pebble conglomerate is the diagnostic lithology further southeast. Unit OEml$_c$ varies in color from gray, olive gray, and greenish gray to very dark gray. Weathering colors are generally medium to dark gray.

Unit OEml$_c$ includes parts of unit Twoc of Tabor and Cady (1978a) and is equivalent to unit Tocc of Snavely and others (1993).

Unit OEml$_c$ apparently has conformable relations with coeval units OEm and OEm$_o$. The age of unit OEml$_c$ is poorly constrained as Oligocene to Early Eocene by zircon fission-track minimum dates from adjacent, conformable rocks. Conglomerates of unit OEml$_c$ are interpreted as channel-fill facies (Snavely and others, 1993).

VOLCANOGENIC ROCKS

~~M~~vb **Basaltic rocks of the Juan de Fuca plate, subsurface only (Miocene)**—Unit ~~M~~vb is inferred to be composed of basaltic rocks extruded along the Juan de Fuca Ridge. Drill data from the ridge indicate compositions similar to those of other mid-oceanic ridges, but detailed chemical analysis indicates a heterogenous mantle source (Van Wagoner and Leybourne, 1991).

The age of unit ~~M~~vb under the coastline is greater than 8 Ma as determined from magnetic isochron 4.5 (Atwater and Severinghaus, 1989). This unit is depicted only on Figure 5.

Evb **Basaltic rocks (Eocene)**—Unit Evb is composed mainly of altered basaltic breccia and conglomerate with lesser amounts of basalt, pillow basalt, and felsic tuff (Stewart, 1970; Tabor and Cady, 1978a). All exposures in the Forks quadrangle are discontinuous pods that are associated with coastal mélanges or the Clearwater River fault [shear zone]. Larger exposures within these shear zones are mapped as unit Evb, but small pods and phacoids occur throughout these mé-

langes and are mapped as part of unit MEbx (Stewart, 1970; Rau 1975, 1979; Tabor and Cady, 1978a).

Unit Evb is predominantly basalt, but analyses of samples from the Salmon River sheet directly southeast of the Forks quadrangle (Lingley and others, 1996) suggest that these basaltic rocks represent two different tectonic or geochemical environments: (1) mid-oceanic ridge basalt and (2) oceanic or seamount alkalic basalt. Some, but not all, of these rocks have chemistries that are essentially indistinguishable from those of typical Crescent Formation basalts (Lingley and others, 1996), which have been interpreted as a margin-rift basin volcanic sequence (Babcock and others, 1994). However, one of the samples is alkalic basalt similar to the volcanics of Grays River (Phillips and others, 1989), which were erupted into a fore-arc setting (Walsh and others, 1987).

The juxtaposition of disparate basalt chemistries within gouge along the Salmon River thrust fault [shear zone] suggests either considerable fault offset along shears or that some of the basalts are exotic blocks (Lingley and others, 1996).

The age of unit Evb is poorly constrained. Stratiform deposits southeast of the Forks quadrangle have conformable contacts with rocks of unit MEm$_r$, suggesting a Miocene to Late Eocene age. Crescent Formation basalt chemistry implies an early Eocene age.

Felsic tuffs identified and dated by Richard Stewart (University of Washington, written commun., 1999) crop out directly west of Yahoo Lake and along Prairie Creek southeast of the Forks quadrangle. The tuffs yield an Early Miocene (22 ma) zircon fission-track minimum age, but these tuffs probably are unconformable on the basaltic rocks.

Most exposures of unit Evb lie in contact with tectonic breccias of unit MEbx. Unit Evb is inferred to be in fault contact with units Mm$_r$, Mml, MEm$_r$, MEml, and MEm.

Unit Evb may be equivalent to unit Tb of Tabor and Cady (1978a) and Lingley and others (1996); however, the limited areal extent of the these rocks precludes reliable correlation. Many workers (Applegate, 1989; Tabor and Cady, 1978b; Stewart, 1970) correlate unit Evb with the Crescent Formation basalts (unit Evc), which crop out south of the Forks quadrangle.

MIXED SEDIMENTARY AND VOLCANIC ROCKS

MEbx **Tectonic breccia and intensely sheared siliciclastic rocks (Miocene to Eocene)**—Unit MEbx includes two basic lithologic associations: (1) mélanges injected along fault planes or as piercement structures and (2) thick sequences of intensely sheared marine sedimentary rocks associated with northeast-striking high-angle faults or northwest-striking thrust faults. Unit MEbx also includes those coastal areas where sea stacks of randomly varying lithology and metamorphic grade lie in close proximity (and apparent disequilibrium) with each other.

The matrix of unit MEbx mélanges consists of very dark clay and lesser amounts of sheared admixtures of thin-bedded sandstone, siltstone, and shale similar to those of unit MEm$_r$ and volcanogenic rocks similar to unit Evb. The clay is silty and commonly petroliferous (Snavely and Kvenvolden, 1989; Palmer and Lingley, 1989, Lingley and von der Dick, 1991). The clay has a distinctive, penetrative, scaley cleavage that is parallel with the faults that bound these units or forms a concentric pattern in map view (Orange, 1990). In the sheared sedimentary rocks, the cleavage is oriented subparallel with the lithologic layering and wraps around sandstone phacoids. Sandstones within unit MEbx, which range from granules to boulders several tens of meters across, are lithofeldspathic arenites similar to those of units Mml, MEml, and OEm, but randomly oriented bedding indicates that these are either exotic blocks or rotated phacoids. Volcanogenic rocks within unit MEbx are mostly chloritized volcaniclastic conglomerates or various basaltic lithologies. The volcanogenic rocks are all exotic and range from granules to boulders. Larger volcanic outcrops are mapped separately as unit Evb.

Structural relations within the mélanges indicate they were injected as diapiric muds along strike-slip or thrust faults or as piercement structures (Rau and Grocock, 1974; Orange, 1990, 1991). Sheared marine sedimentary rocks mapped as unit MEbx are interpreted as unusually thick sections of fault gouge.

The matrix of unit MEbx mélanges is mostly lower Miocene, whereas the exotic blocks range from Middle Eocene to Lower Miocene. The only Eocene faunas recovered from the Coastal sheet are from unit MEbx. Volcanic clasts recovered from unit MEbx southeast of the Forks quadrangle had chemistries representative of Crescent Formation basalts (Lingley and others, 1996), which also suggests an Eocene age for part of unit MEbx. Unit MEbx is equivalent to unit Thm of Rau (1975, 1979) and Lingley and others (1996) and parts of unit Tom of Snavely and Kvenvolden (1989). Unit MEbx includes the Clearwater and Salmon River shear zones of Stewart (1970), the Duck Creek diapir of Rau and Grocock (1974), and various mélange zones as mapped by Rau (1975, 1979) and Snavely and Kvenvolden (1989).

Unit MEbx is in fault contact with adjacent rocks, except in the sheared sedimentary rocks of the Salmon River shear zone southeast of the Forks quadrangle where it grades upward into unit MEm.

QUATERNARY DEPOSITIONAL ENVIRONMENTS AND CHRONOLOGY

The landforms of the Olympic Peninsula have been strongly influenced over the past two million years or more by repeated alpine and continental glaciations. The easily eroded rocks and rapid uplift of the Olympic Mountains provided, and continue to provide, large volumes of sediment for transport downvalley by glaciers and free-flowing rivers. The west-flowing rivers of the peninsula are incised into the thick sequences of sedimentary fill, forming terraces and, in places, also exposing the underlying bedrock. Deposits of dense till, coarse outwash gravels, glaciolacustrine silts and clays, localized peats, and capping and interbedded deposits of loess, indicate the range of glacial and periglacial environments that once occupied these valleys.

The thick sequences of valley-fill deposits found on the western Olympic Peninsula offer some opportunities for palynological and radiocarbon dating. Because of their large ba-

sin areas and headwater elevations (originating in the Mount Olympus massif) compared to other west-flowing drainages, the Hoh and Queets valleys provide the most comprehensive and well-preserved depositional record of climatic events on the peninsula's west side. Therefore, Thackray's work in these basins serves well to represent a glacial chronology specific to the western Olympic Peninsula. Based on his work and building on that of earlier mappers to the north and south (Heusser, 1964, 1969, 1973a,b, 1974, 1978; Crandell, 1964, 1965; Moore, 1965), he postulates that there were at least four major advances of alpine glaciers, several of which had readvances, occurring over the past one million years or so.

Stagnating glaciers that persisted through the waning stages of glacial advances commonly left hummocky surfaces with small closed basins (kettles) underlain by a complex combination of stratified and unstratified till, fine sands, silts, and clays. The kettles and other areas of ponding developed peats as they filled with organic deposits. Such features, seen in the lower Queets valley and in the Hoh valley for several miles upstream of the Hoh oxbow, are associated with recession of the alpine glaciers and mapped as units $Qapwt_2$ and Qat in the respective valleys. These features are also present in the continental glacial deposits north of the town of Forks, where the deposits are collectively mapped as till (unit Qgt).

Interglacial periods were characterized by erosion in the upper areas of the drainage basins and relatively low rates of sedimentation in the lowland areas. Thick, often extensive, deposits of peat, some of which are now exposed in coastal bluffs, were laid down during these times (Heusser, 1964; Thackray, 1996). These nonglacial deposits, variable in thickness, generally represent much longer time intervals than the coarser, rapidly deposited glacial sediments. They have been mildly folded and help document the timing of recent tectonic deformation (Thackray, 1996; Thackray and Pazzaglia, 1994; McCrory, 1997; Thackray, 1998). Much less extensive peat deposits formed during the waning stages of glaciations, both upvalley and downvalley of moraines. Radiocarbon ages from these deposits have been used to constrain the ages of glaciations that deposited the moraines (Heusser, 1964; Thackray, 1996).

Deposits left by the Juan de Fuca lobe of the continental ice sheet have yielded only a limited number of radiocarbon dates on the Olympic Peninsula. Based on radiocarbon samples collected from within and just north of the Forks quadrangle, we correlate these deposits to the most recent major advance, the Vashon Stade (~14,000–12,000 yr B.P.) of the Fraser Glaciation (Schasse, in progress; this study).

Along and within the Dickey and Sol Duc River channels, thick deposits of outwash contain rock types foreign to the Olympic Peninsula, indicating a remote continental-glacial source. These deposits are reworked and mixed with alpine outwash and other fluvial deposits in the Quillayute valley and in the lower reaches of the Calawah and Bogachiel Rivers, two of its tributaries. The North Fork Calawah River provides an excellent example of an underfit stream occupying what was a prominent outwash channel from the continental Juan de Fuca lobe. The outwash gravels in this valley (mapped as unit Qgo) are very coarse and permeable, allowing much of the North Fork to flow subsurface.

Adjacent to the Sol Duc and Dickey River outwash channels, continental glacial deposits are represented by extensive dense lodgement till and unconsolidated ablation till. The ablation till is characterized by hummocky topography underlain by discontinuous lenses of stratified sands and gravels and small pockets of silts and clays. This 'dead-ice terrain' and similar landforms left by melting alpine ice are mapped in most places as drift.

Based on the radiocarbon ages reported from the peninsula and elsewhere in the Pacific Northwest, the last continental and alpine glacial advances were probably not synchronous (Porter, 1964; Gillespie and Molnar, 1995; this study and references within). This is not surprising considering the differences in accumulation areas, elevation ranges, orographic influences, and therefore, response times of the glaciers to climatic change. Furthermore, glacial deposits of the western Olympic Peninsula seem to record more frequent advances than those recognized in the Cascade Range to the east, suggesting a greater sensitivity of Olympic Mountains glaciers to regional climatic fluctuations. The response behavior of these glaciers might be due both to the strong marine influence and the low gradient of the peninsula's west-flowing rivers. The low valley gradient would allow small changes in the equilibrium-line altitude to correspond to relatively large changes in accumulation areas.

Asynchronous fluctuations in sediment input from continental and alpine glaciers resulted in repeated reworking of alluvial deposits, particularly in the lowland area surrounding Forks. The result is a complex stratigraphic record with buried, incised, and inset geomorphic features such as terraces and moraines. One such example of this geomorphic relationship is the interfluve ridge northwest of Forks (mapped as unit $Qapw_2$).

For this compilation, we carried Thackray's chronology northward over the rest of the map area into the Bogachiel, Calawah, and Sol Duc basins, assuming that climatic conditions (precipitation and temperature) would be generally comparable from north to south along the western peninsula. Thackray's chronology was modified slightly to accommodate established state map symbology and to conform to published 1:100,000-scale geologic maps for Washington

For compilation of the Forks quadrangle, the Quaternary stratigraphic record has been divided into six time-stratigraphic and origin-based units: older pre-Wisconsinan alpine glacial, younger pre-Wisconsinan alpine glacial, pre-Fraser alpine glacial, Fraser alpine glacial, Fraser (Vashon) continental glacial, and Holocene outwash and alluvium. Each group includes some or all of the following types of deposits—till, outwash, lacustrine, and undivided drift. Thackray's map units are landform units. They are converted here to material units (that is, end moraine to till) but their original map representation should not be overlooked.

We map the younger of Thackray's drifts, the middle and late Wisconsinan Hoh Oxbow and Twin Creeks drifts, as units Qat or Qao. We map his early Wisconsinan Lyman Rapids drift as unit Qapo, Qapt, or Qap. His two pre-Wisconsinan units, the Wolf Creek and Whale Creek drifts, are mapped as units $Qapwo_1$, $Qapwt_1$, and $Qapwo_2$, $Qapwt_2$, $Qapw_2$, respectively.

Deposits of loess are found overlying and interbedded with the various glacial deposits discussed above. These vary in thickness and degree of weathering. Thicker and more clay-rich loess deposits are generally found associated with the older glacial deposits, with thinner and siltier loess capping the younger glacial deposits. The loess deposits are generally less than 2 m thick and are mentioned in a number of the unit descriptions but not mapped as a separate unit.

STRUCTURE

Structure within the Forks quadrangle consists mainly of north- to northwest-striking, east-dipping strata that have been folded and imbricated by northwest-trending thrust faults (Plate 1).

Most macroscopic folds trend northwest. In the eastern portion of the Forks quadrangle, bedrock is disrupted by a weakly developed northwest-trending cleavage, which is subparallel with lithologic layering. As noted above, three major structural sheets, which probably ride on three major thrust fault systems, have been tentatively identified (Figs. 4 and 5).

All of the aforementioned structures are cut by younger northeast-trending faults, which are apparently vertical and have strike-slip displacement (Rau, 1979). Quaternary sediments are also deformed, resulting in several generations of wave-cut and fluvial terraces. Moderate-angle dips and broad folding reflect several meters of episodic uplift and indicate ongoing tectonism (Glover, 1940b; Moore, 1965; Rau, 1973, 1980; Thackray and Pazzaglia, 1994; Thackray, 1998).

Major Faults

Mapping major faults in the western Olympic Peninsula is a daunting task because regional faults, where exposed, are characterized by unusually wide shear zones (Rau 1975, 1979; Orange and others, 1993; Lingley and others, 1996) that in some places grade laterally into undeformed strata. Broad northwest- or northeast-trending valleys with thick rain forest vegetation have formed in most of these shear zones, and, as a result, discrete fault planes are seldom exposed.

These difficulties notwithstanding, two major sets of structures have been mapped: (1) northwest-trending structures interpreted as thrust faults (Stewart, 1970; Rau, 1975, 1979; Tabor and Cady, 1978a,b; Snavely, 1987; Orange and others, 1993; Lingley and others, 1996) and northeast-trending structures interpreted as high-angle strike-slip faults (Reagan, 1909; Rau 1975, 1979; Palmer and Lingley, 1989; Orange, 1990). Criteria used to map the traces of these large-scale faults include linear valleys, sheared strata, localized penetrative cleavage, and mélange zones. Linear magnetic anomalies parallel the northwest-trending shear zones north of the Hoh River (Carol Finn, U.S. Geological Survey, written commun., 1989), suggesting that the anomalies are caused by buried thrust slivers of volcanic rocks, possibly unit Evb (Fig. 5). Basaltic units are the most widely distributed rocks on the Olympic Peninsula that have high magnetic susceptibility. Major lithologic packets are abruptly truncated by the northeast-trending high-angle faults. (See the Clearwater River fault [shear zone] on Fig. 4 and Stewart, 1970). Significant mismatches in faunal assemblages, ages, and in zircon fission-track minimum ages are also present across the northwest-trending faults.

The Huelsdonk thrust separates unit OEm on the Huelsdonk sheet from Miocene and Eocene rocks on the Salmon River sheet. It was mapped and named the Huelsdonk shear zone and interpreted as a thrust fault on the basis of kinematic indicators by Stewart (1970). Part of the Huelsdonk thrust has been named the 'Bogachiel thrust fault' (Rau, 1979), but that name is not used herein because a different fault probably parallels the Bogachiel River valley more closely.

The Salmon River thrust separates Miocene to Eocene rocks (units ~~M~~Em, ~~M~~Em$_r$, ~~M~~Eml, and ~~M~~Eml$_c$) on the Salmon River sheet from Miocene rocks of the Hoh lithic assemblage on the Coastal sheet (units ~~M~~m$_r$, ~~M~~ml, and ~~M~~ml$_c$). This fault is well constrained by zircon fission-track minimum age dates and structural relations near the North Fork Salmon River. New zircon fission-track ages confirm a west-verging thrust plane in that location. The Salmon River thrust fault is exposed along Shale Creek (Stewart, 1970). While the extension of this structure further to the northwest is required by stratigraphic relations, the position of this extension is uncertain. The position used herein has been chosen on the basis of unexplained stratigraphic truncations shown on Tabor and Cady (1978a) south of Nolan Creek and poor zircon fission-track minimum age control. We have tentatively linked it to the May Hill fault of Rau (1979). However, the west edge of the Salmon River sheet could be located farther west along Miller Creek or farther east near Mount Octopus.

The coastal thrust faults were originally mapped by the alignment of unit ~~M~~Ebx outcrops along the coast and on numerous coastal islands (Tabor and Cady, 1978a,b; Rau, 1979). This structure is interpreted as a pair of thrusts faults that coalesce at depth. (See Figure 5.) The eastern thrust is exposed as a discontinuous series of thrust fault segments between the Quillayute and Hoh Rivers (Rau, 1979). The western thrust fault consists of an offshore feature that exposes unit ~~M~~Ebx on islands shown in Tabor and Cady (1978a,b).

These coastal thrusts separate a section chiefly composed of Miocene rocks of the Hoh lithic assemblage on the Coastal sheet from thick Pliocene–Miocene sediments of the Quillayute Formation (unit ~~PM~~m) offshore. Snavely and Kvenvolden (1989) reinterpreted the coastal thrust faults as a west-dipping, eastward-verging thrust, partly on the basis of micropaleontology by Weldon Rau. Rau cannot support this use of the data (DGER, oral commun., 1988), nor do the kinematic indicators of Orange (1990). Therefore we follow the original mapping, but acknowledge the possibility that Snavely and Kvenvolden may be correct.

Thrusting appears to have developed as a spasmodic east-to-west progression. This progression may have begun during the Late Eocene or Early Oligocene. Thrusting continued in the coastal parts of the quadrangle with erosional truncation along a 14 Ma old regional unconformity (Boyer and Lingley, 1991; Palmer and Lingley, 1989). Rapid uplift of coastal areas described in Rau (1973, 1980), Moore (1965), and Thackray (1998) probably results from ongoing imbrication of the accretionary prism (Boyer and Lingley, 1991) or northward translation of the Juan de Fuca plate (McCrory, 1996).

The northeast-trending high-angle faults cut the northwest-trending thrust faults and are of probable late Miocene to Recent age (Palmer and Lingley, 1989). These include the Goodman Creek and Hoh River faults of Rau (1979) and the Clearwater River shear zone [fault] of Stewart (1970). Vertical cleavage within the fault zones (Orange, 1990), the relation of fault traces to topography, and analogy to the well-constrained northeast-trending vertical fault at Ocean City (Palmer and Lingley, 1989) indicate that the northeast-trending structures have vertical fault planes. Rau (1979) interprets these as strike-slip faults. These faults may have formed in response to northward translation and right-lateral step-over of the Juan de Fuca plate as it passed through the restraining bend formed by Vancouver Island. (See Tabor, 1975).

Lithologic Layering

Lithologic layering in the study area is generally defined by the alternating light-colored, medium- to thick-bedded sandstone and darker, laminated or thin-bedded, very fine-grained sandstone, siltstone, shale, and slate. Monolithologic sections thicker than a few tens of meters are not present, and even the volcanogenic sequences display considerable lithologic heterogeneity. Sole marks and dewatering features are common, but cross-beds and graded bedding are rare. In general, primary sedimentary structures are well preserved. Partial and complete

Bouma sequences are locally developed, especially in the vicinity of the village of Kalaloch, where they are interbedded with massive sandstone beds that are several meters thick. Because most of the stratigraphic succession in the Forks quadrangle is composed of monotonous lithofeldspathic sandstone, bedding characteristics are more useful for mapping than petrography.

Thin- to medium-bedded rocks (units Mm$_r$ and MEm$_r$, together with large parts of units MEm and OEm) comprise about 75 percent of exposed Tertiary strata. Typically, these rocks are laminated and bedded on a scale of 0.5 mm to about 20 cm. Most display sharp, laterally extensive contacts with little or no change in bed thickness over distances of hundreds (to thousands?) of meters and no change in thickness within individual outcrops. Some of the thin-bedded strata have been called rhythmites by previous workers (Rau, 1976; Tabor, 1975; Tabor and Cady, 1978a), hence the designations Mm$_r$ and MEm$_r$ used in this report.

Sequences mapped as thick-bedded (parts of units Mml, MEml, MEm, OEm, Mml$_c$, and MEml$_c$) are composed of massive or banded, multistory sandstones, with individual bed thicknesses ranging from 0.3 to 5 meters, together with intervening sections similar to the thin-bedded rocks. These sequences range in thickness from about 10 to 45 m and commonly have parallel or lenticular (scoured) contacts. These thick-bedded packets are laterally discontinuous owing to scoured contacts and (or) lenticular or tabular geometries among multistory packets.

In the Huelsdonk sheet, bedding generally strikes west-northwest and dips steeply to the northeast. Bedding here forms part of the northern limb of 'big horseshoe' (Tabor, 1975), an eastward-plunging antiform that covers most of the central and eastern Olympic Peninsula and controls the trend of the major ridges. In the northern and southern Salmon River sheet, lithologic layering strikes mostly northwest and dips steeply northeast. In the central portion, south of the Clearwater River shear zone, it strikes northeast. Attitudes of lithologic layering in these two domains are consistent with those generated by southwest-verging thrust faults. In the Coastal sheet, rocks of the Hoh lithic assemblage generally strike northward, but much of the bedding is disrupted by macroscopic folding and diapiric clay intrusions associated with unit MEbx.

Cleavage

In the eastern parts of Huelsdonk and Salmon River sheets, bedding is cut by a locally developed cleavage. This cleavage is nearly coplanar with bedding in soft units MEm$_r$ and OEm, but steeper in the massive sandstones of units Mml, MEml, and OEm. The cleavage is interpreted as resulting from strain transmitted from the thrusting process. In several locations throughout the Olympic Mountains, cleavage is penetratively developed on the hanging walls, directly above the major thrust planes, but cleavage development progressively diminishes at stratigraphically higher levels.

In the western Huelsdonk and Salmon River sheets and in the coastal sheet, shearing is limited to zones of scaly cleavage associated with fault gouge or diapirs (unit MEbx). Many sandstone beds are sheared out, forming phacoids. The cleavage appears to wrap around and rotate many of these phacoids. In some areas, bedding has been thoroughly rearranged by shearing and is indistinguishable from scaly cleavage. Most cleavage is thought to have formed in response to thrust faulting and mimics the shape of the underlying major thrust planes. Orange (1990) noted that cleavage in the northeast-trending shear zones is planar and aligned parallel with the bounding fault(s), whereas concentric steeply dipping foliation is present around piercement structures.

Folds

Macroscopic folds in the study area (Fig. 4) mostly trend northwest, but west- or southwest-trending folds are present near the coast (Rau, 1975, 1979). The largest folds have amplitudes of several hundred meters and wave lengths of more than two kilometers. They are mostly open concentric folds, but overturned and nearly isoclinal folds are also present.

Fold patterns and geometries are consistent with thrust-driven folding. These structures include leading-edge or ramp anticlines, piggyback basins (Boyer and Lingley, 1994), or other thrust-related folds, most of which developed perpendicular to the Juan de Fuca–North American plate convergence vector. However, some fold axes are subparallel with the convergence vector (for example, the Kalaloch Ridge syncline of Rau (1975) and the Kalaloch syncline of Thackray (1998).

Mesoscopic folds are fairly common throughout the study area. Most have an open-concentric geometry and bend both bedding and, where present, cleavage. Axial planes are generally subparallel with bedding, and fold axes plunge northwest or southeast at shallow to moderate angles. Folds are frequently associated with small faults, either as drag or rollover features.

RELIABILITY OF BEDROCK MAPPING

Poor exposure, complex structure, and monotonous stratigraphy have resulted in mapping that has an unusually high degree of uncertainty. A paucity of radiometric age dates and reliance on the imprecise zircon fission-track dates or on microfaunal assemblages, which may be diachronous, compound the uncertainty.

ACKNOWLEDGMENTS

Bill Phillips (Univ. of Edinburgh), Glenn Thackray (Univ. of Idaho), Scott Babcock, Dave Engebretson, and Kevin Kelly (Western Washington Univ.), and Josh Logan, Tim Walsh, and Hank Schasse (DGER) provided insight and important geological data. Leslie Lingley (Leslie Geological Services) provided much information on the geology of the Salmon River drainage. Helpful reviews were provided by Rowland Tabor (USGS), Glenn Thackray, Matt Brunengo (DNR), Dick Stewart (Univ. of Washington), and DGER staff members Eric Schuster, Weldon Rau, Jari Roloff, and Karen Meyers. Eric Schuster digitized the map, and Jari Roloff, Keith Ikerd, and Anne Heinitz of DGER's editorial and cartographic staff prepared the diagrams.

This study was partially funded with grants from the Minerals Management Service as part of the Continental Margins Program (subagreement nos. 14-12-0001-30387, 14-35-0001-30497, and 14-35-0001-30643), USGS STATEMAP (contract no. 98HQAG2062), and Olympic Natural Resources Center (contract nos. UW 234153 and DNR FY96-165). We thank Cathy Dunkel of Minerals Management Service and Linda Miller of the Texas Bureau of Economic Geology for their assistance and support, and Karl Wegmann and Dave Parks for field support in collecting samples in remote areas for radiocarbon dating. We also thank DNR Olympic Region staff for logistical field support and Olympic National Park for providing accommodations during a large portion of this field work.

REFERENCES CITED

Addicott, W. O., 1976, Neogene molluscan stages of Oregon and Washington. *In* Fritsche, A. E.; Ter Best, Harry, Jr.; Wornardt, W. W., editors, The Neogene symposium—Selected technical papers on paleontology, sedimentology, petrology, tectonics and geologic history of the Pacific coast of North America: Society of Economic Paleontologists and Mineralogists Pacific Section, 51st Annual Meeting, p. 95-115.

Applegate, J. D. R., 1989, An upper plate origin for basalt blocks in the Cenozoic subduction complex of the Olympic Mountains, northwest Washington State: Yale University Bachelor of Science thesis, 1 v.

Atwater, Tanya; Severinghaus, Jeff, 1989, Tectonic maps of the northeast Pacific. *In* Winterer, E. L.; Hussong, D. M.; Decker, R. W., editors, The eastern Pacific Ocean and Hawaii: Geological Society of America DNAG Geology of North America, v. N, p. 15-20, plates 3B and 3C.

Babcock, R. S.; Suczek, C. A.; Engebretson, D. C., 1994, The Crescent "terrane", Olympic Peninsula and southern Vancouver Island. *In* Lasmanis, Raymond; Cheney, E. S., convenors, Regional geology of Washington State: Washington Division of Geology and Earth Resources Bulletin 80, p. 141-157.

Bouma, A. H.; Brouwer, A., editors, 1964, Turbidites: Elsevier Publishing Company Developments in Sedimentology 3, 264 p.

Boyer, S. E.; Lingley, W. S., Jr., 1991, Structure and kinematics of the Olympic subduction complex, NW Washington, and implications for mechanical models of accretionary prisms [abstract]: Geological Society of America Abstracts with Programs, v. 23, no. 5, p. A428.

Boyer, S. E.; Lingley, W. S., Jr., 1994, A model for the structural evolution of parts of the Olympic subduction complex and associated piggyback basins [abstract]: Geological Society of America Abstracts with Programs, v. 26, no. 7, p. A-188.

Brandon, M. T., 1996, Probability density plot for fission-track grain-age samples: Radiation Measurements, v. 26, no. 5, p. 663-676.

Brandon, M. T.; Calderwood, A. R., 1990, High-pressure metamorphism and uplift of the Olympic subduction complex: Geology, v. 18, no. 12, p. 1252-1255.

Brandon, M. T.; Vance, J. A., 1992, Tectonic evolution of the Cenozoic Olympic subduction complex, Washington State, as deduced from fission track ages for detrital zircons: American Journal of Science, v. 292, no. 8, p. 565-636.

Brown, K. M.; Orange, D. L., 1993, Structural aspects of diapiric mélange emplacement—The Duck Creek diapir: Journal of Structural Geology, v. 15, no. 7, p. 831-847.

Crandell, D. R., 1964, Pleistocene glaciations of the southwestern Olympic Peninsula, Washington: U.S. Geological Survey Professional Paper 501-B, p. B135-B139.

Crandell, D. R., 1965, The glacial history of western Washington and Oregon. *In* Wright, H. E., Jr.; Frey, D. G., editors, The Quaternary of the United States: Princeton University Press, p. 341-353.

Dickinson, W. R., 1970, Interpreting detrital modes of graywacke and arkose: Journal of Sedimentary Petrology, v. 40, no. 2, p. 695-707.

Dieu, Julie; Shelmerdine, Bill, 1997, Module A—Sedimentation assessment. *In* Pentec Environmental, Inc., North Fork Calawah watershed analysis, watershed administrative unit 200315—Final report: Pentec Environmental, Inc. [under contract to] Rayonier Timberlands Operating Company, 1 v.

Easterbrook, D. J.; Briggs, N. D.; Westgate, J. A.; Gorton, M. P., 1981, Age of the Salmon Springs glaciation in Washington: Geology, v. 9, no. 2, p. 87-93.

Easterbrook, D. J.; Crandell, D. R.; Leopold, E. B., 1967, Pre-Olympia Pleistocene stratigraphy and chronology in the central Puget Lowland, Washington: Geological Society of America Bulletin, v. 78, no. 1, p. 13-20.

Fiksdal, A. J.; Brunengo, M. J., 1980, Forest Slope Stability Project, Phase I: Washington Department of Ecology Technical Report 80-2a, 18 p., 7 plates.

Galbraith, R. F., 1988, Graphical display of estimates having differing standard errors: Technometrics, v. 30, no. 3, p. 271-281.

Gerstel, W. J., 1997, Progress report on the geologic mapping and landslide inventory of the west-central portion of the Olympic Peninsula, Washington: Washington Geology, v. 25, no. 4, p. 30-32.

Gerstel, W. J., 1999, Deep-seated landslide inventory of the west-central Olympic Peninsula: Washington Division of Geology and Earth Resources Open File Report 99-2, 36 p., 2 plates.

Gillespie, Alan; Molnar, Peter, 1995, Asynchronous maximum advances of mountain and continental glaciers: Reviews of Geophysics, v. 33, no. 3, p. 311-364.

Glover, S. L., 1940a, Browns Point Formation, Olympic Peninsula, Washington [abstract]: Geological Society of America Bulletin, v. 51, no. 12, part 2, p. 2022-2023.

Glover, S. L., 1940b, Pleistocene deformation in the Olympic coastal region, Washington: Northwest Science, v. 14, no. 3, p. 69-71.

Grady, M. T., 1985, Stratigraphy, sedimentology, and hydrocarbon potential of the Hoh turbidite sequence (Miocene), western Olympic Peninsula, Washington: University of Idaho Master of Science thesis, 192 p.

Heusser, C. J., 1964, Palynology of four bog sections from the western Olympic Peninsula, Washington: Ecology, v. 45, no. 1, p. 23-40.

Heusser, C. J., 1969, Modern pollen spectra from the Olympic Peninsula, Washington: Torreya, v. 96, no. 4, p. 407-417.

Heusser, C. J., 1973a, Age and environment of allochthonous peat clasts from the Bogachiel River valley, Washington: Geological Society of America Bulletin, v. 84, no. 3, p. 797-804.

Heusser, C. J., 1973b, Environmental sequence following the Fraser advance of the Juan de Fuca Lobe, Washington: Quaternary Research, v. 3, no. 2, p. 284-306.

Heusser, C. J., 1974, Quaternary vegetation, climate, and glaciation of the Hoh River valley, Washington: Geological Society of America Bulletin, v. 85, no. 10, p. 1547-1560.

Heusser, C. J., 1978, Palynology of Quaternary deposits of the lower Bogachiel River area, Olympic Peninsula, Washington: Canadian Journal of Earth Sciences, v. 15, no. 10, p. 1568-1578.

Heusser, C. J.; Heusser, L. E.; Peteet, D. M., 1999, Humptulips revisited—A revised interpretation of Quaternary vegetation and climate of western Washington, USA: Palaeogeography, Palaeoclimatology, Palaeoecology, v. 150, no. 3-4, p. 191-221.

Koch, A. J., 1968, Petrology of the "Hoh Formation" of Tertiary age in the vicinity of the Raft River, western Washington: University of Washington Master of Science research paper, 41 p., 1 plate.

Kvenvolden, K. A.; Golan-Bac, Margaret; Snavely, P. D., Jr., 1989a, Composition of natural gases in seeps, outcrops, and a test well. *In* Preliminary evaluation of the petroleum potential of the Tertiary accretionary terrane, west side of the Olympic Peninsula, Washington: U.S. Geological Survey Bulletin 1892, p. 37-45.

Kvenvolden, K. A.; Rapp, J. B.; Hostettler, F. D.; Snavely, P. D., Jr.,1989b, Comparison of molecular markers in oil and rock extracts. *In* Preliminary evaluation of the petroleum potential of the Tertiary accretionary terrane, west side of the Olympic Peninsula, Washington: U.S. Geological Survey Bulletin 1892, p. 19-35.

Lingley, L. L., in press, Watershed analysis of the Salmon River: Leslie Geological Services, 1 v.

Lingley, W. S., Jr., 1995, Preliminary observations on marine stratigraphic sequences, central and western Olympic Peninsula, Washington: Washington Geology, v. 23, no. 2, p. 9-20.

Lingley, W. S., Jr.; Logan, R. L.; Walsh, T. J.; Gerstel, W. J.; Schasse, H. W., 1996, Reconnaissance geology of the Matheny Ridge–Higley Peak areas, Olympic Peninsula, Washington: Washington Division of Geology and Earth Resources [contract report], 31 p., 1 plate.

Lingley, W. S., Jr.; von der Dick, Hans, 1991, Petroleum geochemistry of Washington—A summary: Washington Geology, v. 19, no. 4, p. 23-27.

Logan, R. L., in progress, Geologic map of the Copalis Beach 1:100,000 quadrangle, Washington: Washington Division of Geology and Earth Resources Open File Report.

Long, W. A., 1975, Glacial studies on the Olympic Peninsula: U.S. Forest Service, 1 v., 9 plates.

Long, W. A., 1976, Glacial geology of the Olympic Peninsula, Washington: U.S. Forest Service, 135 p.

McClellan, P. H.; Snavely, P. D., Jr., 1987, Multichannel seismic-reflection profiles collected in 1976 off of the Washington–Oregon coast: U.S. Geological Survey Open-File Report 87-607, 2 p., 1 plate.

McClellan, P. H.; Snavely, P. D., Jr., 1988, Multichannel seismic-reflection profiles collected in 1980 off of the Washington and northern Oregon coast: U.S. Geological Survey Open-File Report 88-205, 4 p., 1 plate.

McCrory, P. A., 1996, Tectonic model explaining divergent contraction directions along the Cascadia subduction margin, Washington: Geology, v. 24, no. 10, p. 929-932.

McCrory, P. A., 1997, Evidence for Quaternary tectonism along the Washington coast: Washington Geology, v. 25, no. 4, p. 14-20.

McFarland, C. R., 1983, Oil and gas exploration in Washington, 1900–1982: Washington Division of Geology and Earth Resources Information Circular 75, 119 p.

Moore, J. L., 1965, Surficial geology of the southwestern Olympic Peninsula: University of Washington Master of Science thesis, 63 p., 1 plate.

Munsell Color Corporation, 1975, Munsell soil color charts: Munsell Color Corporation, 3-ring binder edition.

Orange, D. L., 1990, Criteria helpful in recognizing shear-zone and diapiric mélanges—Examples from the Hoh accretionary complex, Olympic Peninsula, Washington: Geological Society of America Bulletin, v. 102, no. 7, p. 935-951.

Orange, D. L., 1991, The effects of fault zones and fluid flow on the structural, hydrologic and geomorphic evolution of accretionary complexes—Examples from Cascadia: University of California, Santa Cruz Doctor of Philosophy thesis, 140 p.

Orange, D. L.; Geddes, D. S.; Moore, J. C., 1993, Structural and fluid evolution of a young accretionary complex—The Hoh rock assemblage of the western Olympic Peninsula, Washington: Geological Society of America Bulletin, v. 105, no. 8, p. 1053-1075.

Orange, D. L.; Underwood, M. B., 1995, Patterns of thermal maturity as diagnostic criteria for interpretation of mélanges: Geology, v. 23, no. 12, p. 1144-1148.

Palmer, R. H., 1927a, Geology and petroleum possibilities of the Olympic Peninsula, Washington: American Association of Petroleum Geologists Bulletin, v. 11, no. 12, p. 1321-1328.

Palmer, R. H., 1927b, The Hoh formation of Washington: Journal of Geology, v. 35, no. 3, p. 276-278.

Palmer, S. P.; Lingley, W. S., Jr., 1989, An assessment of the oil and gas potential of the Washington outer continental shelf: University of Washington, Washington Sea Grant Program, Washington State and Offshore Oil and Gas, 83 p., 12 plates.

Pazzaglia, F. J.; Brandon, M. T., 1996, Tectonic implications of fluvial terraces along the Clearwater River, Olympic Mountains, Washington. *In* Friends of the Pleistocene, Quaternary glaciation and tectonism on the western Olympic Peninsula, Washington: Friends of the Pleistocene, 50 p.

Phillips, W. M.; Walsh, T. J.; Hagen, R. A., 1989, Eocene transition from oceanic to arc volcanism, southwest Washington. *In* Muffler, L. J. P.; Weaver, C. S.; Blackwell, D. D., editors, Proceedings of workshop XLIV—Geological, geophysical, and tectonic setting of the Cascade Range: U.S. Geological Survey Open-File Report 89-178, p. 199-256.

Porter, S. C., 1964, Composite Pleistocene snow line of Olympic Mountains and Cascade Range, Washington, Geological Society of America Bulletin, v. 75, no. 5, p. 477-482.

Rau, W. W., 1973, Geology of the Washington coast between Point Grenville and the Hoh River: Washington Division of Geology and Earth Resources Bulletin 66, 58 p.

Rau, W. W., 1975, Geologic map of the Destruction Island and Taholah quadrangles, Washington: Washington Division of Geology and Earth Resources Geologic Map GM-13, 1 sheet, scale 1:63,360.

Rau, W. W., 1979, Geologic map in the vicinity of the lower Bogachiel and Hoh River valleys, and the Washington coast: Washington Division of Geology and Earth Resources Geologic Map GM-24, 1 sheet, scale 1:62,500.

Rau, W. W., 1980, Washington coastal geology between the Hoh and Quillayute Rivers: Washington Division of Geology and Earth Resources Bulletin 72, 57 p.

Rau, W. W.; Grocock, G. R., 1974, Piercement structure outcrops along the Washington coast: Washington Division of Geology and Earth Resources Information Circular 51, 7 p.

Rau, W. W.; McFarland, C. R., 1982, Coastal wells of Washington: Washington Division of Geology and Earth Resources Report of Investigations 26, 4 sheets.

Reagan, A. B., 1909, Some notes on the Olympic Peninsula, Washington: Kansas Academy of Science Transactions, v. 22, p. 131-238.

Schasse, H. W., in progress, Geologic map of the Cape Flattery 1:100,000 quadrangle, Washington: Washington Division of Geology and Earth Resources Open File Report.

Schuster, J. E., 1994, Progress on the state geologic map: Washington Geology, v. 22, no. 3, p. 39-42.

Shaw, S. C., 1995, Habitat conservation plan workshop—Reports to the Board of Natural Resources: Washington Department of Natural Resources unpublished report, 1 v.

Shaw, S. C.; Vaugeois, L. M., 1999, Comparison of GIS-based models of shallow landsliding for application to watershed management: Washington Department of Natural Resources [for the] Timber, Fish, Wildlife Program TFW-PR10-99-001, 104 p.

Silver, E. A., 1972, Pleistocene tectonic accretion of the continental slope off Washington: Marine Geology, v. 13, no. 4, p. 239-249.

Snavely, P. D., Jr., 1987, Tertiary geologic framework, neotectonics, and petroleum potential of the Oregon–Washington continental margin. *In* Scholl, D. W.; Grantz, Arthur; Vedder, J. G., compilers and editors, Geology and resources potential of the continental margin of western North America and adjacent ocean basins—Beaufort Sea to Baja California: Circum-Pacific Council for Energy and Mineral Resources, Earth Science Series, v. 6, p. 305-335.

Snavely, P. D., Jr.; Kvenvolden, K. A., 1989, Geology and hydrocarbon potential. *In* Preliminary evaluation of the petroleum potential of the Tertiary accretionary terrane, west side of the Olympic Peninsula, Washington: U.S. Geological Survey Bulletin 1892, p. 1-17, 1 plate.

Snavely, P. D., Jr.; MacLeod, N. S.; Niem, A. R.; and others, 1993, Geologic map of the Cape Flattery, Clallam Bay, Ozette Lake, and Lake Pleasant quadrangles, northwestern Olympic Peninsula, Washington: U.S. Geological Survey Miscellaneous Investigations Series Map I-1946, 1 sheet, scale 1:48,000.

Snavely, P. D., Jr.; Wagner, H. C., 1982a, Geologic cross section across the continental margin of southwestern Washington: U.S. Geological Survey Open-File Report 82-459, 10 p., 1 plate.

Snavely, P. D., Jr.; Wagner, H. C., 1982b, Geophysical data collected on the southern Washington continental shelf along line 12, USGS R/V S.P. Lee cruise 3-76: U.S. Geological Survey Open-File Report 82-424, 1 sheet.

Stewart, R. J., 1970, Petrology, metamorphism and structural relations of graywackes in the western Olympic Peninsula, Washington: Stanford University Doctor of Philosophy thesis, 123 p., 5 plates.

Stewart, R. J., 1974, Zeolite facies metamorphism of sandstone in the western Olympic Peninsula, Washington: Geological Society of America Bulletin, v. 85, no. 7, p. 1139-1142.

Tabor, R. W., 1975, Guide to the geology of Olympic National Park: University of Washington Press, 144 p., 2 plates.

Tabor, R. W.; Cady, W. M., 1978a, Geologic map of the Olympic Peninsula, Washington: U.S. Geological Survey Miscellaneous Investigations Series Map I-994, 2 sheets, scale 1:125,000.

Tabor, R. W.; Cady, W. M., 1978b, The structure of the Olympic Mountains, Washington—Analysis of a subduction zone: U.S. Geological Survey Professional Paper 1033, 38 p.

Thackray, G. D., 1996, Glaciation and neotectonic deformation on the western Olympic Peninsula, Washington: University of Washington Doctor of Philosophy thesis, 139 p., 2 plates.

Thackray, G. D., 1998, Convergent-margin deformation of Pleistocene strata on the Olympic coast of Washington, USA. *In* Stewart, I. S.; Vita-Finze, C., editors, Coastal tectonics: Geological Society [of London] Special Publications, 146, p. 199-211.

Thackray, G. D.; Pazzaglia, F. J., 1994, Quaternary stratigraphy, tectonic geomorphology, and fluvial evolution of the western Olympic Peninsula, Washington. *In* Swanson, D. A.; Haugerud, R. A., editors, Geologic field trips in the Pacific Northwest: University of Washington Department of Geological Sciences, v. 2, p. 2A 1–2A 29.

Van Wagoner, N. A.; Leybourne, M. I., 1991, Evidence for magma mixing and a heterogeneous mantle on the West Valley segment of the Juan de Fuca Ridge: Journal of Geophysical Research, v. 96, no. B10, p. 16,295-16,318.

Walsh, T. J.; Korosec, M. A.; Phillips, W. M.; Logan, R. L.; Schasse, H. W., 1987, Geologic map of Washington—Southwest quadrant: Washington Division of Geology and Earth Resources Geologic Map GM-34, 2 sheets, scale 1:250,000, with 28 p. text.

Weaver, C. E., 1916, The Tertiary formations of western Washington: Washington Geological Survey Bulletin 13, 327 p., 6 plates.

Wegmann, K. W., 1999, Late Quaternary fluvial and tectonic evolution of the Clearwater River basin, western Olympic Mountains, Washington State: University of New Mexico Master of Science thesis, 217 p., 4 plates.

Weissenborn, A. E.; Snavely, P. D., Jr., 1968, Summary report on the geology and mineral resources of Flattery Rocks, Quillayute Needles, and Copalis National Wildlife Refuges, Washington: U.S. Geological Survey Bulletin 1260-F, 16 p. ■

Appendix 1. Detrital zircon fission-track ages from the Forks 1:100,000 quadrangle, Washington.

The locations of these samples are shown on Plate 1, which is keyed to Table 1.

Explanation: Ns (the number of spontaneous tracks) is the actual number of fission tracks counted on each zircon grain in a sample, and RhoS is the track density for each zircon crystal, calculated from Ns. Ni (the number of induced tracks) is the actual number of tracks counted on the mica detector image corresponding to each zircon crystal. RhoI is the track density on the mica detector calculated from Ni. Estimates of grain ages, best-fit peaks, and uncertainties are calculated using the programs of Brandon (1996).

All programs and fission-track data used in this study are available from the following website: http://love.geology.yale.edu/~brandon. The relevant programs are ZETAAGE (version 4.7), which calculates “exact” FT ages and confidence intervals, and BINOMFIT (version 1.8), which is an implementation of the binomial peak-fit algorithm of Galbraith (1988). Programs are provided as source code (Quick Basic) and DOS executables.

Sample # WSL 7-98-5 (Laboratory #Z-195)

------ GRAIN AGES ORDERED WITH INCREASING AGE ------

Grain no.	RhoS (cm^-2)	(Ns)	RhoI (cm^-2)	(Ni)	Grain age (Ma) Age	--95% CI--	
1	7.57E+05	(13)	1.16E+06	(20)	18.1	8.2	38.0
2	1.68E+06	(48)	2.30E+06	(66)	20.2	13.6	29.7
3	1.92E+06	(22)	2.44E+06	(28)	21.8	11.9	39.4
4	1.05E+06	(25)	1.30E+06	(31)	22.4	12.6	39.1
5	1.94E+06	(37)	2.25E+06	(43)	23.8	14.9	37.9
6	3.32E+06	(38)	3.23E+06	(37)	28.4	17.6	46.0
7	1.41E+06	(27)	1.36E+06	(26)	28.7	16.1	51.2
8	1.42E+06	(19)	1.27E+06	(17)	30.9	15.2	63.2
9	2.75E+06	(42)	2.23E+06	(34)	34.1	21.2	55.4
10	3.01E+06	(23)	2.36E+06	(18)	35.3	18.3	69.4
11	1.51E+06	(23)	9.82E+05	(15)	42.2	21.2	87.1
12	1.68E+06	(32)	1.05E+06	(20)	44.1	24.5	81.4
13	1.83E+06	(21)	1.13E+06	(13)	44.4	21.4	96.7
14	5.47E+06	(47)	3.03E+06	(26)	49.8	30.3	83.9
15	4.19E+06	(36)	2.10E+06	(18)	55.0	30.6	103.0
16	1.38E+06	(21)	6.55E+05	(10)	57.5	26.2	137.2
17	3.96E+06	(34)	1.63E+06	(14)	66.6	35.1	134.6
18	2.05E+06	(47)	6.98E+05	(16)	80.4	45.2	152.3
POOL	2.00E+06	(555)	1.63E+06	(452)			

----------PARAMETERS FOR BEST-FIT PEAKS----------

{Standard error for peak age includes group error}

{Peak width is for PD plot assuming a kernel factor = 0.60}

PEAK NUMBER	----PEAK AGE & CONF. INTERVAL (MA)---- MEAN	(----63% CI---)		(----95% CI---)		W(Z)	FRAC(%)	SE(%)	COUNT
1)	25.8	(-2.7	+3.0)	(-5.0	+6.3)	0.30	55.1	17.5	9.9
2)	51.9	(-7.3	+8.4)	(-13.3	+17.8)	0.35	44.9	17.5	8.1
						TOTAL:	100.0		18.0

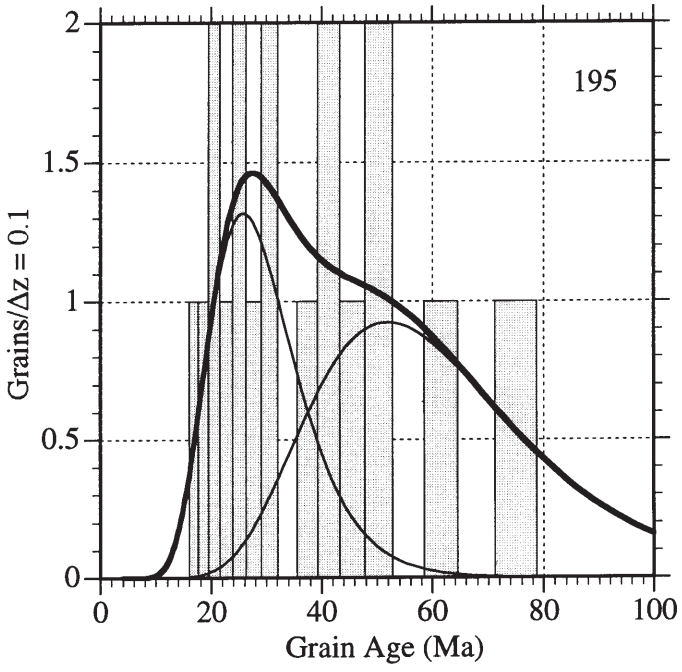

Sample # Stewart 91-72 (Laboratory #Z-143)

```
------ GRAIN AGES ORDERED WITH INCREASING AGE ------
Grain  RhoS     (Ns)    RhoI     (Ni)    Grain age (Ma)
 no.  (cm^-2)          (cm^-2)          Age   --95% CI--
  1  5.59E+05 (  16) 1.12E+06 (  32)  14.7   7.5  27.4
  2  3.20E+06 (  61) 5.97E+06 ( 114)  15.6  11.2  21.5
  3  3.61E+06 (  69) 6.34E+06 ( 121)  16.6  12.2  22.5
  4  3.46E+06 (  66) 5.45E+06 ( 104)  18.5  13.4  25.4
  5  4.19E+06 ( 120) 6.50E+06 ( 186)  18.8  14.9  23.7
  6  4.40E+06 (  84) 6.76E+06 ( 129)  18.9  14.3  25.0
  7  3.88E+06 (  74) 5.97E+06 ( 114)  18.9  13.9  25.6
  8  5.94E+05 (  17) 9.08E+05 (  26)  19.1   9.7  36.5
  9  4.98E+06 ( 114) 7.42E+06 ( 170)  19.5  15.3  24.8
 10  2.44E+06 (  56) 3.54E+06 (  81)  20.2  14.1  28.7
 11  5.59E+06 ( 128) 7.77E+06 ( 178)  20.9  16.6  26.3
 12  5.46E+06 ( 125) 7.55E+06 ( 173)  21.0  16.6  26.5
 13  4.68E+06 ( 134) 6.46E+06 ( 185)  21.1  16.8  26.4
 14  3.18E+06 (  91) 3.95E+06 ( 113)  23.4  17.7  30.9
 16  5.06E+06 ( 145) 6.25E+06 ( 179)  23.6  18.8  29.4
 15  2.97E+06 (  68) 3.67E+06 (  84)  23.6  16.9  32.9
 17  3.63E+06 ( 104) 4.40E+06 ( 126)  24.0  18.4  31.2
 18  5.87E+06 ( 168) 6.74E+06 ( 193)  25.3  20.5  31.2
 19  3.60E+06 (  55) 3.67E+06 (  56)  28.6  19.4  42.3
 20  3.38E+06 (  87) 3.30E+06 (  85)  29.8  21.9  40.7
 21  5.19E+06 (  99) 4.98E+06 (  95)  30.2  22.7  40.1
 22  8.73E+05 (  25) 8.03E+05 (  23)  31.6  17.3  58.3
 23  6.23E+06 ( 119) 5.66E+06 ( 108)  32.0  24.6  41.6
 24  2.37E+06 (  68) 1.36E+06 (  39)  50.6  33.7  77.1
 25  2.41E+06 (  62) 1.32E+06 (  34)  52.9  34.4  83.0
 26  2.62E+06 (  75) 1.33E+06 (  38)  57.2  38.4  87.0
 27  3.67E+06 (  70) 1.68E+06 (  32)  63.4  41.3  99.6
POOL 3.54E+06( 2300) 4.34E+06( 2818)

-----------------------PARAMETERS FOR BEST-FIT PEAKS--------------------------
{Standard error for peak age includes group error}
{Peak width is for PD plot assuming a kernel factor =  0.60}
PEAK   ----PEAK AGE & CONF. INTERVAL (MA)---- PEAK WIDTH --GRAINS IN PEAK----
NUMBER   MEAN (----63% CI---) (----95% CI---)    W(Z)    FRAC(%) SE(%)  COUNT
  1)     22.1 (  -0.8   +0.8) (  -1.6   +1.7)    0.16      85.0    6.9   22.9
  2)     55.6 (  -5.7   +6.3) ( -10.5  +13.0)    0.24      15.0    6.9    4.1
                                                  TOTAL: 100.0          27.0
```

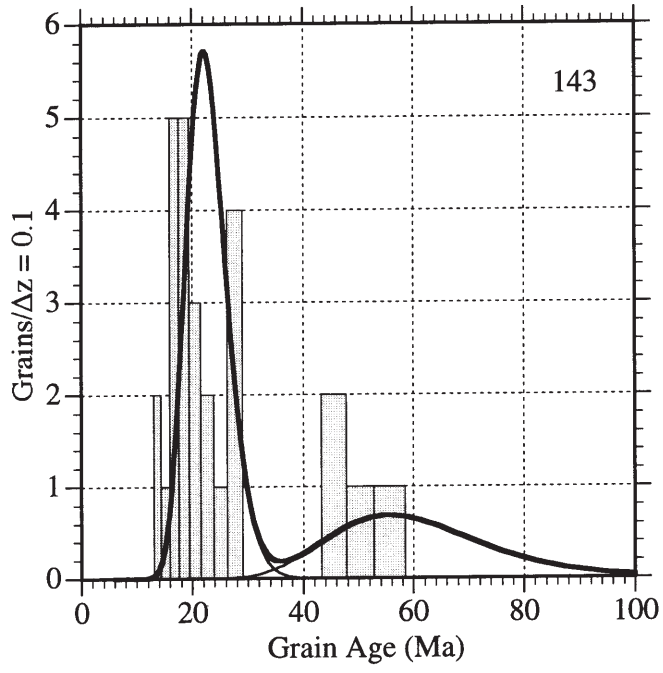

Sample # Stewart 94-15 (Laboratory #Z-162)

------ GRAIN AGES ORDERED WITH INCREASING AGE ------

Grain no.	RhoS (cm^-2)	(Ns)	RhoI (cm^-2)	(Ni)	Grain age (Ma) Age	--95% CI--	
1	1.42E+06	(34)	3.39E+06	(81)	12.5	8.1	18.8
2	1.09E+06	(26)	2.14E+06	(51)	15.1	9.0	24.6
3	9.64E+05	(23)	1.76E+06	(42)	16.2	9.3	27.5
4	1.63E+06	(39)	2.93E+06	(70)	16.5	10.8	24.7
5	1.05E+06	(16)	1.77E+06	(27)	17.6	8.8	33.7
6	1.09E+06	(26)	1.80E+06	(43)	17.9	10.5	29.8
7	2.03E+06	(58)	2.97E+06	(85)	20.2	14.2	28.5
8	2.68E+06	(41)	3.86E+06	(59)	20.6	13.4	31.1
9	1.84E+06	(44)	2.56E+06	(61)	21.3	14.1	31.9
10	7.57E+05	(13)	9.89E+05	(17)	22.7	10.1	49.3
11	1.09E+06	(26)	1.22E+06	(29)	26.5	15.0	46.6
12	2.10E+06	(50)	2.10E+06	(50)	29.5	19.6	44.6
13	1.09E+06	(26)	6.29E+05	(15)	50.9	26.1	103.5
POOL	1.45E+06	(422)	2.16E+06	(630)			

----------PARAMETERS FOR BEST-FIT PEAKS----------

{Standard error for peak age includes group error}

{Peak width is for PD plot assuming a kernel factor = 0.60}

PEAK NUMBER	----PEAK AGE & CONF. INTERVAL (MA)---- MEAN	(----63% CI---)		(----95% CI---)		PEAK WIDTH W(Z)	--GRAINS IN PEAK---- FRAC(%)	SE(%)	COUNT
1)	19.8	(-1.3	+1.4)	(-2.4	+2.8)	0.26	100.0	0.0	13.0
						TOTAL:	100.0		13.0

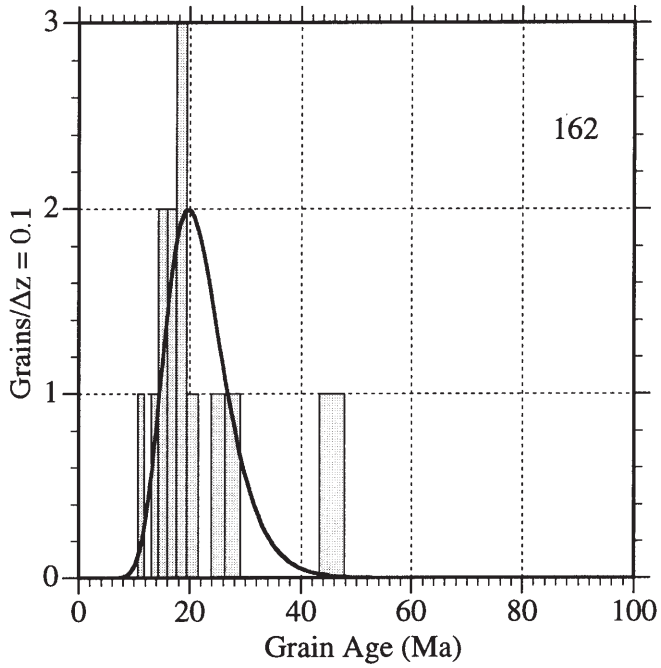

Sample # Stewart 93-4 (Laboratory #Z-152)

------ GRAIN AGES ORDERED WITH INCREASING AGE ------

Grain no.	RhoS (cm^-2)	(Ns)	RhoI (cm^-2)	(Ni)	Grain age (Ma) Age	--95% CI--		P(X2) (%)	Sum age (Ma) Age	--95% CI--	
1	9.22E+05	(22)	9.64E+05	(23)	28.8	15.3	54.0	100.0	28.8	15.3	54.0
2	3.47E+06	(53)	3.60E+06	(55)	29.0	19.5	43.1	98.3	28.9	20.8	40.3
3	3.35E+05	(8)	3.35E+05	(8)	30.1	9.9	91.6	99.7	29.0	21.2	39.7
4	1.44E+06	(33)	1.31E+06	(30)	33.1	19.6	56.1	97.7	30.0	23.1	38.9
5	1.64E+06	(25)	1.44E+06	(22)	34.2	18.5	63.5	98.6	30.6	24.1	38.9
6	1.72E+06	(23)	1.50E+06	(20)	34.6	18.2	66.3	99.2	31.1	24.9	38.9
7	8.80E+05	(21)	7.54E+05	(18)	35.0	17.8	69.7	99.6	31.5	25.5	38.9
8	1.13E+06	(27)	9.64E+05	(23)	35.3	19.5	64.4	99.8	32.0	26.2	39.0
9	2.10E+06	(32)	1.70E+06	(26)	37.0	21.4	64.6	99.8	32.6	27.0	39.2
10	2.10E+06	(32)	1.64E+06	(25)	38.4	22.1	67.6	99.8	33.1	27.8	39.6
11	1.42E+06	(34)	1.09E+06	(26)	39.3	22.9	68.1	99.8	33.7	28.5	39.9
12	1.48E+06	(34)	1.05E+06	(24)	42.5	24.5	74.9	99.6	34.4	29.3	40.5
13	4.71E+06	(72)	3.14E+06	(48)	45.0	30.9	66.3	97.9	35.9	30.9	41.7
14	3.09E+06	(59)	1.89E+06	(36)	49.2	32.0	76.6	93.8	37.2	32.2	42.8
15	2.14E+06	(51)	1.30E+06	(31)	49.3	31.0	79.8	90.5	38.1	33.2	43.6
16	1.00E+06	(23)	5.67E+05	(13)	52.9	25.9	113.7	89.8	38.5	33.7	44.1
17	3.61E+06	(69)	1.99E+06	(38)	54.4	36.2	83.2	78.8	39.8	35.0	45.3
19	2.62E+06	(40)	1.31E+06	(20)	59.8	34.3	108.1	69.9	40.7	35.9	46.1
18	3.61E+06	(62)	1.80E+06	(31)	59.9	38.4	95.4	55.3	41.8	37.0	47.2
20	2.68E+06	(64)	1.26E+06	(30)	63.8	40.9	102.1	38.5	43.0	38.2	48.4
21	2.68E+06	(41)	1.18E+06	(18)	68.0	38.5	125.9	29.6	43.8	39.0	49.3
22	2.68E+06	(41)	1.05E+06	(16)	76.3	42.3	145.9	18.6	44.8	39.9	50.2
23	2.36E+06	(36)	7.86E+05	(12)	89.0	45.8	188.3	9.4	45.7	40.8	51.1
POOL	2.04E+06	(902)	1.34E+06	(593)				9.4	45.7	40.8	51.1

----------PARAMETERS FOR BEST-FIT PEAKS----------

{Standard error for peak age includes group error}

{Peak width is for PD plot assuming a kernel factor = 0.60}

PEAK NUMBER	MEAN	----63% CI---)	(----95% CI---)	W(Z)	FRAC(%)	SE(%)	COUNT
1)	37.5	(-6.9 +8.4)	(-12.3 +18.3)	0.30	44.3	45.1	10.2
2)	52.8	(-7.7 +9.0)	(-14.0 +19.0)	0.29	55.7	45.1	12.8
				TOTAL:	100.0		23.0

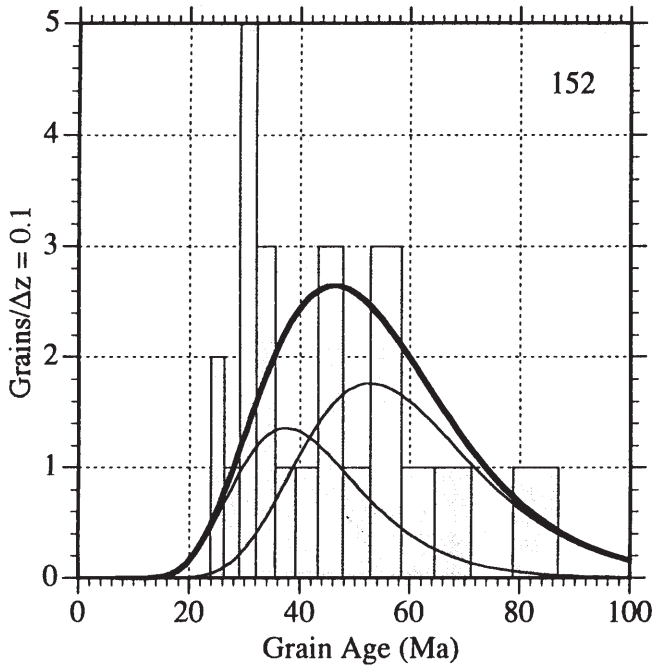

Sample # Stewart 93-49 (Laboratory #Z-178)

------ GRAIN AGES ORDERED WITH INCREASING AGE ------

Grain no.	RhoS (cm^-2)	(Ns)	RhoI (cm^-2)	(Ni)	Grain age (Ma) Age	--95% CI--		P(X2) (%)	Sum age (Ma) Age	--95% CI--	
1	5.45E+05	(13)	6.70E+05	(16)	23.7	10.4	52.2	100.0	23.7	10.4	52.2
2	1.09E+06	(26)	1.26E+06	(30)	25.2	14.3	44.0	88.8	24.6	15.7	38.6
3	3.27E+06	(50)	3.27E+06	(50)	29.0	19.2	43.8	84.7	26.8	20.0	35.8
4	2.88E+06	(33)	2.44E+06	(28)	34.2	20.1	58.7	80.4	28.5	22.1	36.7
5	9.22E+05	(22)	7.54E+05	(18)	35.4	18.2	70.0	84.6	29.3	23.2	37.1
6	1.90E+06	(29)	1.51E+06	(23)	36.5	20.5	66.1	86.1	30.4	24.4	37.7
7	2.44E+06	(28)	1.75E+06	(20)	40.5	22.1	75.9	83.7	31.5	25.6	38.6
8	3.38E+06	(29)	1.98E+06	(17)	49.3	26.3	95.6	68.8	33.0	27.2	40.0
9	3.01E+06	(46)	1.64E+06	(25)	53.2	32.1	90.4	42.6	35.2	29.4	42.2
10	3.80E+06	(58)	1.83E+06	(28)	59.8	37.6	97.6	16.8	37.9	32.0	44.9
11	1.55E+06	(37)	6.70E+05	(16)	66.6	36.4	128.3	8.9	39.6	33.7	46.6
12	4.66E+06	(40)	1.98E+06	(17)	67.7	37.8	127.6	4.8	41.3	35.3	48.3
13	7.60E+06	(116)	2.95E+06	(45)	74.4	52.5	107.5	0.3	45.8	39.7	52.9
16	3.97E+06	(53)	1.42E+06	(19)	80.2	47.1	143.7	0.1	47.7	41.5	54.8
14	3.67E+06	(42)	1.31E+06	(15)	80.4	44.1	156.3	0.1	49.1	42.8	56.2
15	1.70E+06	(26)	5.89E+05	(9)	82.5	38.0	200.8	0.0	49.9	43.6	57.1
17	2.75E+06	(42)	7.20E+05	(11)	109.0	55.9	235.0	0.0	51.6	45.2	58.9
POOL	2.58E+06	(690)	1.45E+06	(387)				0.0	51.6	45.2	58.9

----------PARAMETERS FOR BEST-FIT PEAKS----------

{Standard error for peak age includes group error}

{Peak width is for PD plot assuming a kernel factor = 0.60}

PEAK NUMBER	MEAN	----63% CI---)	(----95% CI---)	W(Z)	FRAC(%)	SE(%)	COUNT
1)	32.3	(-3.8 +4.3)	(-7.1 +9.0)	0.31	40.3	14.5	6.9
2)	68.7	(-6.5 +7.2)	(-12.2 +14.8)	0.31	59.7	14.5	10.1
				TOTAL:	100.0		17.0

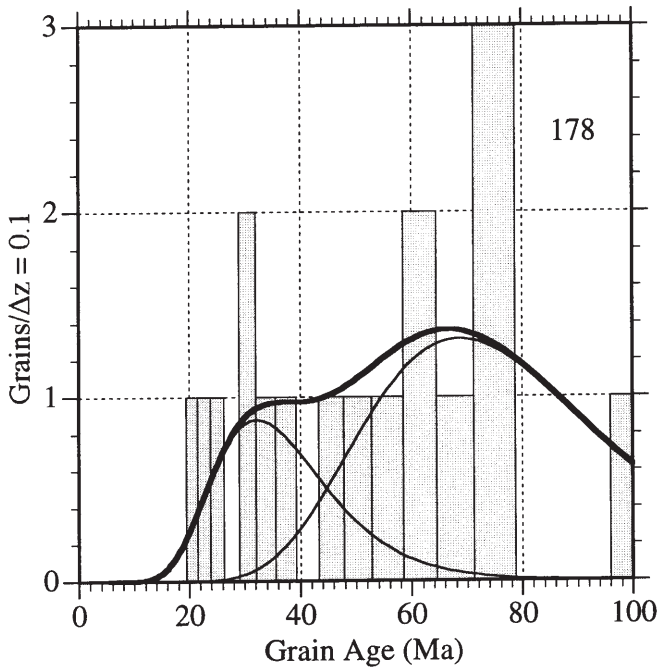

Sample # Stewart 95-13 (Laboratory #Z-170)

```
------ GRAIN AGES ORDERED WITH INCREASING AGE ------
Grain  RhoS     (Ns)     RhoI     (Ni)    Grain age (Ma)
 no.  (cm^-2)           (cm^-2)           Age   --95% CI--
  1  8.15E+05 (  21) 1.90E+06 (  49)  12.6   7.1  21.3
  2  1.30E+06 (  31) 2.47E+06 (  59)  15.4   9.6  24.1
  3  3.77E+05 (   9) 7.12E+05 (  17)  15.6   6.1  36.7
  4  1.01E+06 (  24) 1.63E+06 (  39)  18.0  10.4  30.7
  5  2.35E+06 (  56) 3.65E+06 (  87)  18.8  13.2  26.6
  6  1.85E+06 (  53) 2.58E+06 (  74)  21.0  14.4  30.2
  7  6.70E+05 (  16) 9.22E+05 (  22)  21.3  10.4  42.3
  8  1.26E+06 (  30) 1.72E+06 (  41)  21.4  12.9  35.1
  9  1.40E+06 (  40) 1.85E+06 (  53)  22.1  14.3  33.9
 10  1.38E+06 (  33) 1.80E+06 (  43)  22.5  13.8  36.1
 11  7.54E+05 (  18) 9.64E+05 (  23)  22.9  11.6  44.2
 12  1.40E+06 (  32) 1.70E+06 (  39)  24.0  14.5  39.3
 13  1.01E+06 (  24) 1.22E+06 (  29)  24.2  13.5  43.0
 14  1.30E+06 (  31) 1.55E+06 (  37)  24.5  14.7  40.5
 15  1.09E+06 (  26) 1.30E+06 (  31)  24.5  14.0  42.6
 16  2.10E+06 (  50) 2.47E+06 (  59)  24.8  16.6  36.7
 17  1.63E+06 (  39) 1.89E+06 (  45)  25.3  16.1  39.8
 18  2.24E+06 (  62) 2.35E+06 (  65)  27.9  19.4  40.1
 19  1.22E+06 (  29) 1.26E+06 (  30)  28.2  16.4  48.6
 20  1.61E+06 (  43) 1.65E+06 (  44)  28.6  18.3  44.5
 21  2.47E+06 (  59) 2.30E+06 (  55)  31.3  21.3  46.1
 22  1.96E+06 (  56) 1.75E+06 (  50)  32.7  21.9  48.9
 23  1.97E+06 (  47) 1.72E+06 (  41)  33.5  21.6  52.1
 24  1.84E+06 (  44) 1.55E+06 (  37)  34.7  21.9  55.2
 25  1.51E+06 (  36) 1.26E+06 (  30)  35.0  21.0  58.8
 26  1.13E+06 (  26) 9.17E+05 (  21)  36.1  19.6  67.4
 27  2.60E+06 (  62) 1.80E+06 (  43)  42.0  28.1  63.5
 28  3.39E+06 (  81) 2.26E+06 (  54)  43.7  30.7  62.9
 29  1.61E+06 (  43) 9.35E+05 (  25)  50.0  30.0  85.5
 30  2.10E+06 (  60) 1.15E+06 (  33)  52.9  34.1  83.6
 31  2.88E+06 (  66) 1.48E+06 (  34)  56.5  36.9  88.1
 32  3.10E+06 (  74) 1.55E+06 (  37)  58.2  38.8  88.8
 36  6.29E+05 (  15) 2.93E+05 (   7)  61.7  24.0 179.4
 33  1.51E+06 (  36) 6.70E+05 (  16)  65.2  35.5 126.0
 34  2.85E+06 (  68) 1.26E+06 (  30)  65.8  42.4 104.9
 35  3.39E+06 (  81) 1.38E+06 (  33)  71.3  47.2 110.4
 37  3.06E+06 (  73) 9.64E+05 (  23)  91.8  57.2 153.9
POOL 1.75E+06( 1594) 1.60E+06( 1455)


-----------------------PARAMETERS FOR BEST-FIT PEAKS-------------------------
{Standard error for peak age includes group error}
{Peak width is for PD plot assuming a kernel factor =  0.60}
PEAK   ----PEAK AGE & CONF. INTERVAL (MA)---- PEAK WIDTH --GRAINS IN PEAK----
NUMBER   MEAN (----63% CI---) (----95% CI---)    W(Z)    FRAC(%) SE(%)  COUNT
  1)     24.4 (  -1.3   +1.3) (  -2.4   +2.7)    0.26      69.2    8.3   25.6
  2)     56.1 (  -4.3   +4.6) (  -8.1   +9.5)    0.26      30.8    8.3   11.4
                                                  TOTAL: 100.0           37.0
```

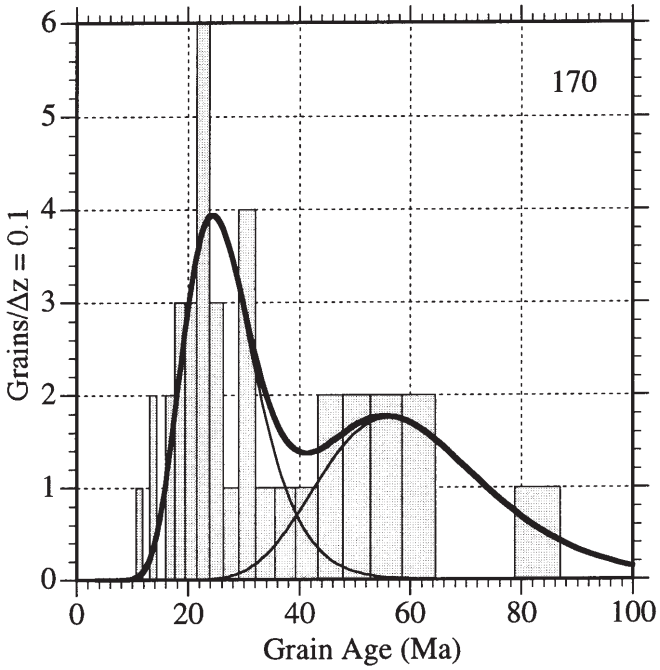
170
Grains/Δz = 0.1
0
1
2
3
4
5
6
0
20
40
60
80
100
Grain Age (Ma)

Sample # Stewart 93-22 (Laboratory #Z-154)

------ GRAIN AGES ORDERED WITH INCREASING AGE ------

Grain no.	RhoS (cm^-2)	(Ns)	RhoI (cm^-2)	(Ni)	Grain age (Ma) Age	--95%	CI--
1	1.30E+06	(31)	3.44E+06	(82)	11.4	7.3	17.4
2	1.76E+06	(42)	3.98E+06	(95)	13.3	9.0	19.3
3	1.59E+06	(38)	3.35E+06	(80)	14.3	9.4	21.3
4	2.88E+06	(77)	5.39E+06	(144)	16.0	12.1	21.2
5	2.35E+06	(56)	4.19E+06	(100)	16.8	11.9	23.6
6	2.81E+06	(67)	4.94E+06	(118)	17.1	12.4	23.2
7	1.09E+06	(26)	1.89E+06	(45)	17.4	10.3	28.7
8	1.68E+06	(40)	2.85E+06	(68)	17.7	11.6	26.5
10	3.94E+06	(94)	6.66E+06	(159)	17.7	13.7	22.9
9	1.38E+06	(33)	2.35E+06	(56)	17.7	11.1	27.7
11	2.76E+06	(79)	4.37E+06	(125)	18.9	14.2	25.1
12	1.24E+06	(32)	1.90E+06	(49)	19.6	12.2	31.2
13	2.26E+06	(54)	3.39E+06	(81)	20.0	13.9	28.6
14	3.35E+06	(80)	4.82E+06	(115)	20.8	15.6	27.8
15	1.47E+06	(35)	2.10E+06	(50)	21.0	13.2	33.0
16	2.03E+06	(58)	2.86E+06	(82)	21.3	14.9	30.1
17	1.76E+06	(42)	2.43E+06	(58)	21.8	14.3	32.9
18	2.51E+06	(60)	3.35E+06	(80)	22.5	15.8	31.9
19	3.10E+06	(74)	4.02E+06	(96)	23.2	16.8	31.7
20	1.38E+06	(33)	1.76E+06	(42)	23.6	14.5	38.1
21	4.40E+06	(126)	5.13E+06	(147)	25.6	20.1	32.7
22	1.77E+06	(44)	1.97E+06	(49)	27.0	17.5	41.3
24	3.04E+06	(87)	2.90E+06	(83)	31.4	23.0	43.0
25	4.57E+06	(109)	4.19E+06	(100)	32.6	24.7	42.8
23	3.86E+06	(92)	3.39E+06	(81)	34.1	25.0	46.5
26	2.51E+06	(60)	2.05E+06	(49)	36.7	24.8	54.7
27	2.26E+06	(54)	1.80E+06	(43)	37.6	24.8	57.5
28	1.22E+06	(29)	9.64E+05	(23)	37.8	21.1	68.3
29	3.69E+06	(88)	2.81E+06	(67)	39.4	28.3	54.9
30	3.14E+06	(81)	2.33E+06	(60)	40.4	28.6	57.5
31	2.43E+06	(58)	1.63E+06	(39)	44.5	29.2	68.6
32	2.77E+06	(66)	1.63E+06	(39)	50.6	33.6	77.3
33	3.23E+06	(77)	1.68E+06	(40)	57.5	38.9	86.6
35	3.56E+06	(85)	1.84E+06	(44)	57.7	39.8	85.1
34	4.69E+06	(112)	2.43E+06	(58)	57.7	41.7	80.8
36	3.73E+06	(89)	1.93E+06	(46)	57.8	40.2	84.5
37	2.77E+06	(66)	1.42E+06	(34)	58.0	37.9	90.5
38	4.23E+06	(101)	2.18E+06	(52)	58.1	41.2	82.8
39	4.57E+06	(131)	2.30E+06	(66)	59.3	43.9	81.1
40	2.43E+06	(58)	1.22E+06	(29)	59.7	37.7	96.8
41	2.64E+06	(63)	1.30E+06	(31)	60.7	39.0	96.6
45	4.44E+06	(106)	2.10E+06	(50)	63.3	44.9	90.6
42	4.65E+06	(111)	2.18E+06	(52)	63.8	45.6	90.5
43	5.20E+06	(124)	2.43E+06	(58)	63.9	46.5	88.9
44	3.77E+06	(90)	1.76E+06	(42)	64.0	44.0	94.7
46	5.28E+06	(141)	2.36E+06	(63)	66.9	49.4	91.5
47	5.80E+06	(166)	2.51E+06	(72)	68.5	51.9	90.5
48	7.42E+06	(177)	2.85E+06	(68)	77.3	58.3	102.3
49	7.67E+06	(183)	2.68E+06	(64)	84.8	63.7	112.8
50	3.23E+06	(77)	9.64E+05	(23)	99.4	62.2	166.1
51	5.27E+06	(151)	1.29E+06	(37)	121.2	84.5	178.6
POOL	3.21E+06	(4053)	2.72E+06	(3434)			

----------PARAMETERS FOR BEST-FIT PEAKS----------

{Standard error for peak age includes group error}

{Peak width is for PD plot assuming a kernel factor = 0.60}

PEAK NUMBER	----PEAK AGE & CONF. INTERVAL (MA)---- MEAN	(----63% CI---)		(----95% CI---)		PEAK WIDTH --GRAINS IN PEAK---- W(Z)	FRAC(%)	SE(%)	COUNT
1)	21.0	(-0.9	+0.9)	(-1.7	+1.9)	0.20	50.6	7.3	25.8
2)	61.5	(-2.7	+2.8)	(-5.2	+5.7)	0.20	49.4	7.3	25.2
						TOTAL:	100.0		51.0

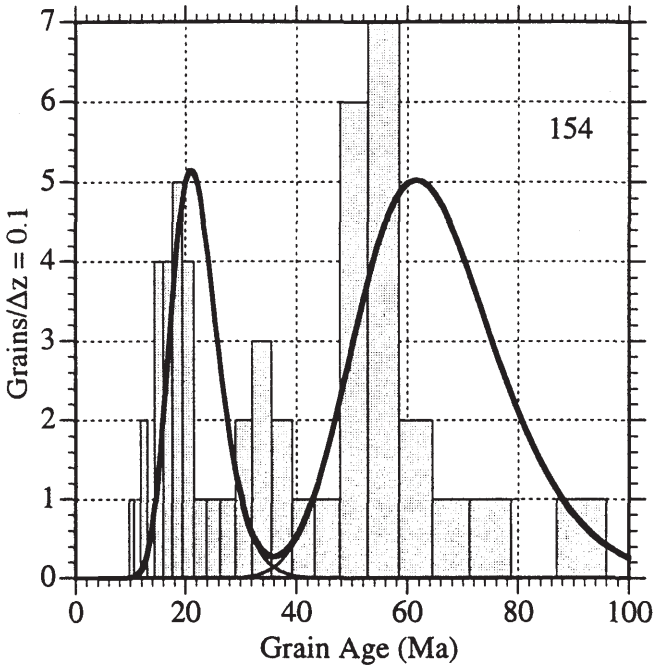
154
Grains/Δz = 0.1
Grain Age (Ma)
0
1
2
3
4
5
6
7
0
20
40
60
80
100

Sample # Stewart 95-11 (Laboratory #Z-169)

------ GRAIN AGES ORDERED WITH INCREASING AGE ------

Grain no.	RhoS (cm^-2)	(Ns)	RhoI (cm^-2)	(Ni)	Grain age (Ma) Age	--95%	CI--
1	8.38E+05	(20)	1.38E+06	(33)	17.8	9.6	31.8
2	1.15E+06	(22)	1.41E+06	(27)	23.9	12.9	43.4
4	1.68E+06	(40)	1.89E+06	(45)	26.0	16.5	40.7
3	6.70E+05	(16)	7.54E+05	(18)	26.0	12.4	53.9
5	1.59E+06	(38)	1.72E+06	(41)	27.1	17.0	43.2
7	1.17E+06	(28)	1.26E+06	(30)	27.3	15.7	47.2
8	1.42E+06	(34)	1.51E+06	(36)	27.6	16.8	45.4
9	1.55E+06	(37)	1.47E+06	(35)	30.9	18.9	50.5
10	7.25E+05	(18)	6.85E+05	(17)	30.9	15.1	63.8
6	1.93E+06	(48)	1.73E+06	(43)	32.6	21.2	50.4
11	1.42E+06	(34)	1.22E+06	(29)	34.2	20.3	58.2
12	1.75E+06	(40)	1.48E+06	(34)	34.4	21.2	55.9
13	2.72E+06	(65)	2.22E+06	(53)	35.8	24.6	52.5
14	1.34E+06	(32)	1.09E+06	(26)	35.9	20.8	62.7
15	1.42E+06	(34)	1.13E+06	(27)	36.7	21.6	63.3
16	1.97E+06	(47)	1.55E+06	(37)	37.1	23.6	58.6
17	1.34E+06	(32)	1.05E+06	(25)	37.3	21.5	65.7
18	1.38E+06	(37)	1.05E+06	(28)	38.5	23.0	65.4
19	1.95E+06	(52)	1.46E+06	(39)	38.9	25.2	60.5
20	1.17E+06	(28)	8.38E+05	(20)	40.8	22.2	76.4
21	3.02E+06	(72)	2.10E+06	(50)	42.0	28.9	61.5
22	1.55E+06	(37)	1.05E+06	(25)	43.1	25.4	74.7
25	1.51E+06	(36)	8.80E+05	(21)	49.9	28.5	90.0
26	2.29E+06	(59)	1.32E+06	(34)	50.5	32.7	79.5
27	2.93E+06	(70)	1.63E+06	(39)	52.3	34.9	79.5
23	1.05E+06	(25)	5.45E+05	(13)	55.8	27.7	118.9
28	3.23E+06	(74)	1.66E+06	(38)	56.7	37.9	86.2
24	1.89E+06	(45)	9.22E+05	(22)	59.4	35.1	104.0
29	2.18E+06	(50)	1.05E+06	(24)	60.5	36.7	103.1
30	2.10E+06	(50)	9.64E+05	(23)	63.1	38.0	108.5
31	1.13E+06	(26)	4.37E+05	(10)	75.0	35.4	174.7
POOL	1.68E+06	(1246)	1.27E+06	(942)			

----------PARAMETERS FOR BEST-FIT PEAKS----------

{Standard error for peak age includes group error}

{Peak width is for PD plot assuming a kernel factor = 0.60}

PEAK NUMBER	MEAN	----63% CI---)	(----95% CI---)	PEAK WIDTH W(Z)	--GRAINS IN PEAK---- FRAC(%)	SE(%)	COUNT
1)	33.0	(-3.3 +3.7)	(-6.1 +7.5)	0.28	60.1	27.4	18.6
2)	48.4	(-7.0 +8.2)	(-12.8 +17.4)	0.28	39.9	27.4	12.4
				TOTAL:	100.0		31.0

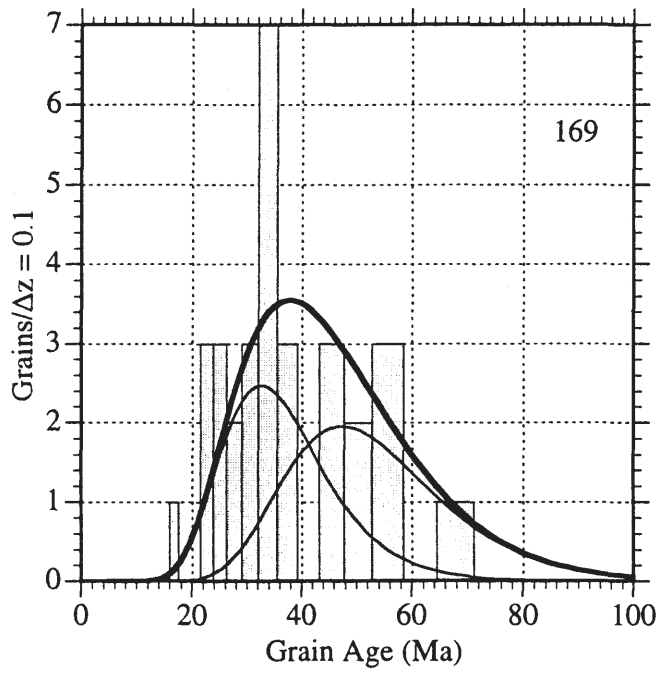

Sample # Hoh-1 (Laboratory #Z-128)

------ GRAIN AGES ORDERED WITH INCREASING AGE ------

Grain no.	RhoS (cm^-2)	(Ns)	RhoI (cm^-2)	(Ni)	Grain age (Ma) Age	--95% CI--	
1	2.05E+06	(49)	2.01E+06	(48)	24.6	16.2	37.4
2	1.93E+06	(46)	1.55E+06	(37)	29.9	19.0	47.5
3	2.62E+06	(40)	1.96E+06	(30)	32.1	19.5	53.4
4	1.98E+06	(34)	1.34E+06	(23)	35.5	20.4	63.2
5	3.01E+06	(46)	1.96E+06	(30)	36.9	22.8	60.5
6	1.96E+06	(30)	1.24E+06	(19)	37.9	20.7	71.4
7	2.62E+06	(40)	1.64E+06	(25)	38.4	22.8	66.2
8	2.88E+06	(44)	1.77E+06	(27)	39.1	23.8	65.8
9	1.63E+06	(28)	9.89E+05	(17)	39.5	21.0	77.1
10	2.44E+06	(35)	1.40E+06	(20)	42.0	23.7	76.9
11	2.68E+06	(41)	1.51E+06	(23)	42.8	25.2	74.8
12	3.47E+06	(53)	1.90E+06	(29)	43.9	27.5	71.7
13	2.55E+06	(39)	1.38E+06	(21)	44.5	25.7	79.8
14	3.73E+06	(57)	1.96E+06	(30)	45.6	28.9	73.6
15	2.75E+06	(42)	1.44E+06	(22)	45.8	26.8	80.7
16	1.77E+06	(27)	9.17E+05	(14)	46.1	23.5	95.5
17	2.95E+06	(45)	1.51E+06	(23)	46.9	27.9	81.4
19	2.23E+06	(32)	1.12E+06	(16)	47.9	25.7	93.7
20	1.51E+06	(36)	7.54E+05	(18)	47.9	26.6	89.8
18	1.51E+06	(36)	7.54E+05	(18)	47.9	26.6	89.8
22	2.65E+06	(38)	1.33E+06	(19)	47.9	27.1	88.2
21	2.75E+06	(42)	1.38E+06	(21)	47.9	27.9	85.4
23	4.13E+06	(63)	2.03E+06	(31)	48.8	31.3	77.7
24	3.34E+06	(51)	1.64E+06	(25)	48.9	29.9	82.5
25	2.88E+06	(44)	1.31E+06	(20)	52.7	30.6	94.5
26	3.46E+06	(66)	1.57E+06	(30)	52.8	33.9	84.3
27	3.01E+06	(46)	1.24E+06	(19)	57.9	33.5	104.9
28	1.83E+06	(28)	7.20E+05	(11)	60.6	29.6	135.5
29	3.67E+06	(56)	1.44E+06	(22)	60.9	36.8	105.0
30	3.93E+06	(60)	1.44E+06	(22)	65.2	39.6	111.9
31	2.62E+06	(40)	9.17E+05	(14)	68.1	36.6	136.0
32	2.62E+06	(45)	8.73E+05	(15)	71.5	39.5	138.5
33	2.49E+06	(38)	6.55E+05	(10)	90.0	44.7	203.4
34	3.99E+06	(61)	9.82E+05	(15)	96.7	54.9	183.6
35	1.94E+06	(37)	4.19E+05	(8)	109.0	50.9	272.0
POOL	2.61E+06	(1515)	1.33E+06	(772)			

----------PARAMETERS FOR BEST-FIT PEAKS----------

{Standard error for peak age includes group error}

{Peak width is for PD plot assuming a kernel factor = 0.60}

PEAK NUMBER	MEAN	----PEAK AGE & CONF. INTERVAL (MA)---- (----63% CI---)	(----95% CI---)	PEAK WIDTH --GRAINS IN PEAK---- W(Z)	FRAC(%)	SE(%)	COUNT
1)	47.2	(-2.3 +2.5)	(-4.5 +5.0)	0.31	100.0	0.0	35.0
				TOTAL:	100.0		35.0

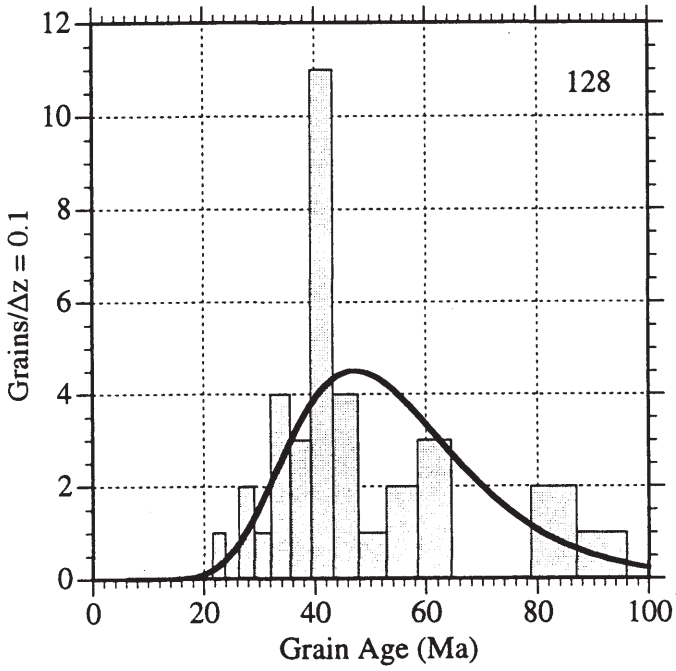

Sample # Bog-1 (Laboratory #Z-94)

------ GRAIN AGES ORDERED WITH INCREASING AGE ------

Grain no.	RhoS (cm^-2)	(Ns)	RhoI (cm^-2)	(Ni)	Grain age (Ma) Age	--95% CI--	
1	1.64E+06	(25)	1.90E+06	(29)	21.2	11.9	37.5
2	2.10E+06	(32)	2.23E+06	(34)	23.2	13.8	38.7
3	1.09E+06	(26)	1.01E+06	(24)	26.7	14.7	48.5
4	1.68E+06	(32)	1.52E+06	(29)	27.1	15.9	46.5
5	2.10E+06	(48)	1.83E+06	(42)	28.1	18.2	43.6
6	1.10E+06	(21)	9.43E+05	(18)	28.7	14.6	57.1
7	2.26E+06	(54)	1.84E+06	(44)	30.2	19.9	46.0
8	1.57E+06	(24)	1.24E+06	(19)	31.0	16.3	59.9
9	1.90E+06	(29)	1.44E+06	(22)	32.4	18.0	59.2
10	1.84E+06	(44)	1.38E+06	(33)	32.8	20.4	53.1
11	1.84E+06	(44)	1.34E+06	(32)	33.8	21.0	55.1
12	1.30E+06	(31)	8.80E+05	(21)	36.2	20.2	66.4
13	1.77E+06	(27)	1.11E+06	(17)	38.9	20.5	76.2
14	3.08E+06	(47)	1.90E+06	(29)	39.8	24.6	65.6
15	2.75E+06	(42)	1.64E+06	(25)	41.2	24.6	70.6
16	2.49E+06	(50)	1.45E+06	(29)	42.3	26.3	69.4
17	2.30E+06	(44)	1.26E+06	(24)	44.9	26.8	77.3
18	2.49E+06	(38)	1.31E+06	(20)	46.5	26.5	84.5
19	1.22E+06	(29)	5.87E+05	(14)	50.6	26.1	103.9
21	2.49E+06	(38)	1.18E+06	(18)	51.6	28.9	96.3
20	2.49E+06	(38)	1.18E+06	(18)	51.6	28.9	96.3
22	1.59E+06	(38)	7.12E+05	(17)	54.6	30.3	103.4
23	2.36E+06	(45)	9.95E+05	(19)	57.9	33.4	105.0
24	2.55E+06	(39)	1.05E+06	(16)	59.5	32.7	114.3
25	2.10E+06	(32)	8.51E+05	(13)	60.0	30.9	124.9
26	1.47E+06	(35)	5.87E+05	(14)	60.9	32.2	123.0
27	1.22E+06	(29)	4.19E+05	(10)	70.4	33.8	162.5
28	1.77E+06	(27)	5.89E+05	(9)	72.7	33.7	176.5
29	1.96E+06	(45)	6.11E+05	(14)	78.2	42.6	154.6
30	1.34E+06	(32)	2.10E+05	(5)	151.9	60.7	499.3
POOL	1.87E+06	(1085)	1.14E+06	(658)			

----------PARAMETERS FOR BEST-FIT PEAKS----------

{Standard error for peak age includes group error}

{Peak width is for PD plot assuming a kernel factor = 0.60}

PEAK NUMBER	----PEAK AGE & CONF. INTERVAL (MA)---- MEAN	(----63% CI---)		(----95% CI---)		PEAK WIDTH W(Z)	--GRAINS IN PEAK---- FRAC(%)	SE(%)	COUNT
1)	32.4	(-3.7	+4.2)	(-6.9	+8.8)	0.30	50.3	22.2	15.1
2)	53.8	(-7.4	+8.5)	(-13.5	+18.0)	0.34	49.7	22.2	14.9
						TOTAL:	100.0		30.0

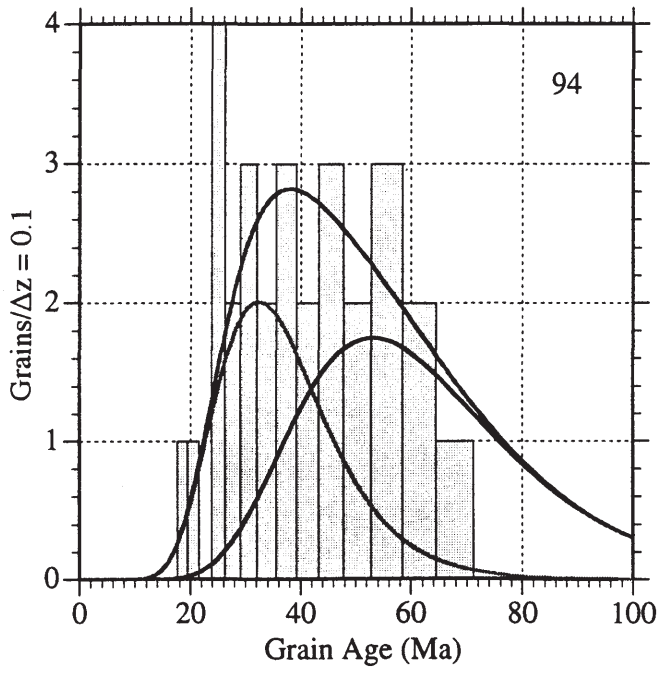

Sample # Stewart 94-42 (Laboratory #Z-167)

------ GRAIN AGES ORDERED WITH INCREASING AGE ------

Grain no.	RhoS (cm^-2)	(Ns)	RhoI (cm^-2)	(Ni)	Grain age (Ma) Age	--95% CI--	
1	2.05E+06	(49)	1.93E+06	(46)	31.2	20.5	47.7
2	1.72E+06	(41)	1.55E+06	(37)	32.5	20.3	52.0
3	2.36E+06	(36)	2.03E+06	(31)	34.0	20.5	56.8
4	1.24E+06	(19)	9.82E+05	(15)	37.0	17.9	78.2
5	1.93E+06	(46)	1.42E+06	(34)	39.6	24.9	63.6
6	2.56E+06	(61)	1.89E+06	(45)	39.7	26.6	59.7
7	1.34E+06	(32)	9.22E+05	(22)	42.5	24.0	76.8
8	1.17E+06	(28)	7.96E+05	(19)	43.0	23.3	81.5
9	1.96E+06	(30)	1.31E+06	(20)	43.8	24.2	81.4
10	1.93E+06	(46)	1.09E+06	(26)	51.6	31.4	87.0
11	1.51E+06	(36)	6.70E+05	(16)	65.4	35.6	126.4
12	2.50E+06	(43)	1.11E+06	(19)	65.8	37.8	119.7
13	1.64E+06	(25)	7.20E+05	(11)	65.9	31.6	148.7
14	3.14E+06	(72)	1.13E+06	(26)	80.5	51.1	131.5
15	4.76E+06	(109)	1.40E+06	(32)	98.9	66.6	151.7
16	3.05E+06	(67)	7.74E+05	(17)	113.9	66.8	207.1
17	2.49E+06	(38)	5.89E+05	(9)	121.2	58.7	285.4
POOL	2.21E+06	(778)	1.21E+06	(425)			

----------PARAMETERS FOR BEST-FIT PEAKS----------

{Standard error for peak age includes group error}

{Peak width is for PD plot assuming a kernel factor = 0.60}

PEAK NUMBER	----PEAK AGE & CONF. INTERVAL (MA)---- MEAN (----63% CI---)	(----95% CI---)	PEAK WIDTH --GRAINS IN PEAK---- W(Z)	FRAC(%)	SE(%)	COUNT
1)	40.2 (-3.4 +3.7)	(-6.4 +7.7)	0.29	65.5	14.3	11.1
2)	89.8 (-11.0 +12.5)	(-20.2 +26.0)	0.30	34.5	14.3	5.9
			TOTAL: 100.0			17.0

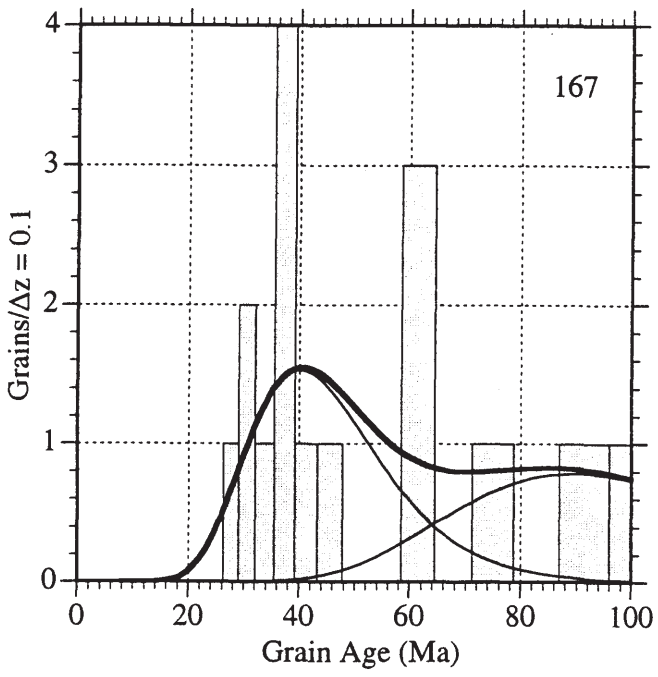

Sample # Stewart 94-41 (Laboratory #Z-189)

Grain no.	RhoS (cm^-2)	(Ns)	RhoI (cm^-2)	(Ni)	Grain age (Ma) Age	--95% CI--	
2	1.17E+06	(28)	1.55E+06	(37)	22.2	13.1	37.3
1	1.17E+06	(28)	1.55E+06	(37)	22.2	13.1	37.3
3	7.54E+05	(18)	8.80E+05	(21)	25.2	12.6	49.5
4	1.44E+06	(22)	1.44E+06	(22)	29.3	15.5	55.4
5	1.01E+06	(24)	9.64E+05	(23)	30.6	16.6	56.6
6	1.78E+06	(34)	1.62E+06	(31)	32.1	19.2	54.0
7	1.89E+06	(45)	1.68E+06	(40)	33.0	21.1	51.8
8	2.18E+06	(52)	1.89E+06	(45)	33.9	22.3	51.6
9	1.38E+06	(33)	1.17E+06	(28)	34.5	20.3	59.3
10	1.36E+06	(26)	1.15E+06	(22)	34.6	18.9	64.0
11	1.26E+06	(24)	1.05E+06	(20)	35.1	18.6	67.0
12	1.90E+06	(29)	1.57E+06	(24)	35.4	19.9	63.5
13	7.86E+05	(15)	6.29E+05	(12)	36.5	16.0	85.4
14	1.38E+06	(33)	1.09E+06	(26)	37.2	21.6	64.7
15	2.10E+06	(32)	1.64E+06	(25)	37.5	21.6	65.9
16	2.86E+06	(41)	2.10E+06	(30)	40.0	24.4	66.3
17	2.16E+06	(33)	1.57E+06	(24)	40.2	23.1	71.1
18	2.42E+06	(37)	1.64E+06	(25)	43.3	25.4	75.0
19	2.75E+06	(42)	1.83E+06	(28)	43.9	26.6	73.5
20	2.01E+06	(48)	1.34E+06	(32)	43.9	27.5	70.9
21	2.01E+06	(48)	1.30E+06	(31)	45.3	28.3	73.6
22	1.83E+06	(28)	1.18E+06	(18)	45.4	24.4	87.2
23	1.70E+06	(26)	1.05E+06	(16)	47.4	24.6	94.6
24	1.64E+06	(25)	9.82E+05	(15)	48.6	24.8	99.2
25	2.03E+06	(58)	1.15E+06	(33)	51.4	33.0	81.3
26	3.08E+06	(47)	1.38E+06	(21)	65.2	38.4	114.9
27	4.40E+06	(63)	1.96E+06	(28)	65.6	41.6	106.4
28	1.94E+06	(37)	8.38E+05	(16)	67.2	36.8	129.6
POOL	1.79E+06	(976)	1.34E+06	(730)			

PARAMETERS FOR BEST-FIT PEAKS

{Standard error for peak age includes group error}
{Peak width is for PD plot assuming a kernel factor = 0.60}

PEAK NUMBER	PEAK AGE & CONF. INTERVAL (MA) MEAN	(----63% CI---)	(----95% CI---)	PEAK WIDTH W(Z)	--GRAINS IN PEAK-- FRAC(%)	SE(%)	COUNT
1)	39.2	(-2.0 +2.2)	(-3.9 +4.3)	0.30	100.0	0.0	28.0
				TOTAL:	100.0		28.0

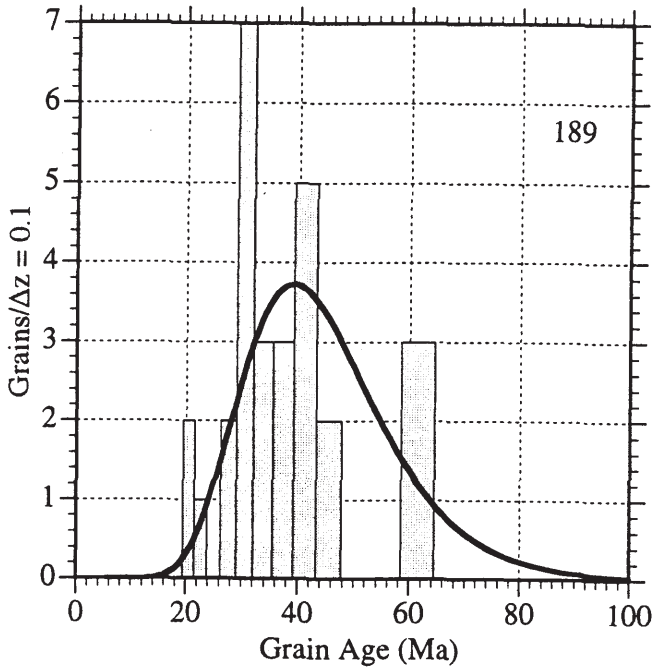

Sample # Stewart 94-40 (Laboratory #Z-166)

------ GRAIN AGES ORDERED WITH INCREASING AGE ------

Grain no.	RhoS (cm^-2)	(Ns)	RhoI (cm^-2)	(Ni)	Grain age (Ma) Age	--95%	CI--
1	1.18E+06	(27)	1.22E+06	(28)	28.3	16.1	49.8
2	4.36E+06	(104)	3.86E+06	(92)	33.0	24.9	43.8
3	2.88E+06	(66)	2.31E+06	(53)	36.5	25.1	53.4
4	2.51E+06	(55)	1.96E+06	(43)	37.5	24.7	57.2
5	2.85E+06	(68)	2.18E+06	(52)	38.3	26.3	56.1
6	1.63E+06	(39)	1.22E+06	(29)	39.4	23.8	66.0
7	4.27E+06	(102)	2.72E+06	(65)	45.9	33.4	63.7
8	3.94E+06	(94)	2.47E+06	(59)	46.6	33.4	65.7
9	3.06E+06	(73)	1.84E+06	(44)	48.5	33.0	72.3
10	3.14E+06	(75)	1.89E+06	(45)	48.8	33.3	72.2
11	3.69E+06	(88)	2.18E+06	(52)	49.5	34.8	71.2
12	3.21E+06	(92)	1.78E+06	(51)	52.8	37.2	75.8
14	1.68E+06	(40)	9.22E+05	(22)	53.1	30.9	93.8
13	4.28E+06	(98)	2.36E+06	(54)	53.1	37.8	75.5
15	2.82E+06	(70)	1.49E+06	(37)	55.3	36.7	84.8
16	2.81E+06	(67)	1.38E+06	(33)	59.3	38.7	92.9
17	2.64E+06	(63)	1.30E+06	(31)	59.3	38.2	94.4
18	3.35E+06	(96)	1.61E+06	(46)	61.0	42.6	88.7
19	2.64E+06	(63)	1.26E+06	(30)	61.3	39.3	98.1
20	2.53E+06	(58)	1.09E+06	(25)	67.6	41.9	112.9
21	1.18E+06	(27)	4.80E+05	(11)	71.2	34.6	159.3
22	2.18E+06	(52)	8.80E+05	(21)	72.1	43.0	126.1
23	1.93E+06	(46)	7.54E+05	(18)	74.3	42.6	136.3
24	1.84E+06	(44)	7.12E+05	(17)	75.2	42.5	140.6
25	1.73E+06	(43)	6.45E+05	(16)	78.1	43.5	148.7
26	3.10E+06	(74)	1.09E+06	(26)	82.8	52.7	135.0
27	2.92E+06	(67)	9.60E+05	(22)	88.5	54.4	150.6
28	3.81E+06	(91)	1.22E+06	(29)	91.3	59.9	143.9
29	2.39E+06	(57)	7.54E+05	(18)	91.9	53.8	166.1
30	2.49E+06	(57)	6.98E+05	(16)	103.2	59.0	192.7
POOL	2.78E+06	(1996)	1.51E+06	(1085)			

----------PARAMETERS FOR BEST-FIT PEAKS----------

{Standard error for peak age includes group error}

{Peak width is for PD plot assuming a kernel factor = 0.60}

PEAK NUMBER	----PEAK AGE & CONF. INTERVAL (MA)---- MEAN	(----63% CI---)	(----95% CI---)	PEAK WIDTH --GRAINS IN PEAK---- W(Z)	FRAC(%)	SE(%)	COUNT
1)	44.6	(-4.7 +5.3)	(-8.8 +11.0)	0.22	48.6	26.7	14.6
2)	69.2	(-10.0 +11.7)	(-18.3 +24.9)	0.27	51.4	26.7	15.4
				TOTAL:	100.0		30.0

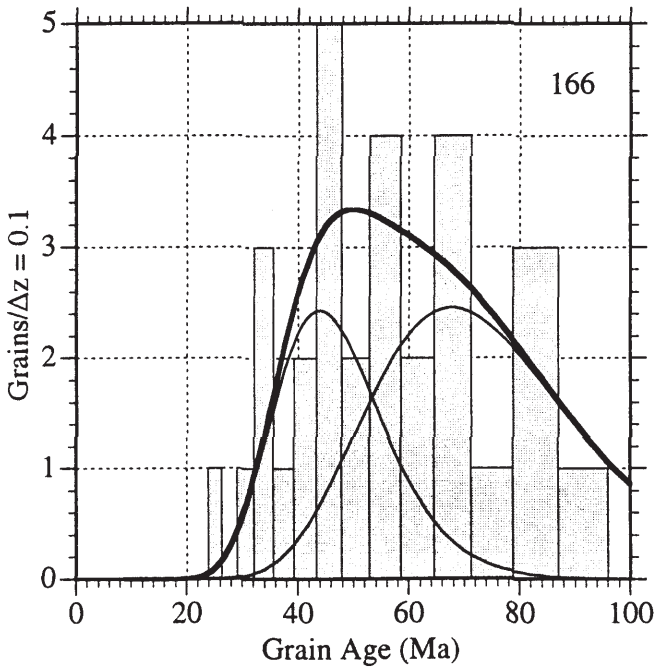

Sample # Arc 88-12 (Laboratory #Z-34; analysis by J. A. Vance, Univ. Washington)

------ GRAIN AGES ORDERED WITH INCREASING AGE ------

Grain no.	RhoS (cm^-2)	(Ns)	RhoI (cm^-2)	(Ni)	Grain age (Ma) Age	--95% CI--	
1	6.08E+06	(175)	3.86E+06	(111)	44.5	35.1	56.5
3	3.26E+06	(135)	1.91E+06	(79)	48.2	36.5	63.6
2	1.11E+07	(244)	6.50E+06	(143)	48.2	39.2	59.4
4	1.12E+07	(171)	6.11E+06	(93)	51.9	40.3	66.8
5	6.92E+06	(199)	3.65E+06	(105)	53.5	42.2	67.8
6	1.31E+07	(255)	6.84E+06	(133)	54.2	43.9	66.9
7	1.79E+07	(303)	8.57E+06	(145)	59.0	48.3	72.0
8	1.24E+07	(178)	5.84E+06	(84)	59.7	46.0	77.4
9	6.22E+06	(179)	2.92E+06	(84)	60.0	46.3	77.8
10	8.27E+06	(266)	3.79E+06	(122)	61.5	49.6	76.3
11	4.41E+06	(153)	1.87E+06	(65)	66.2	49.5	88.4
12	1.78E+07	(332)	6.82E+06	(127)	73.7	60.0	90.5
13	1.00E+07	(306)	3.81E+06	(116)	74.3	60.0	92.1
14	6.79E+06	(201)	2.53E+06	(75)	75.4	57.8	98.2
15	1.23E+07	(261)	4.59E+06	(97)	75.8	60.0	95.7
16	9.76E+06	(256)	3.62E+06	(95)	75.9	59.9	96.0
18	6.41E+06	(206)	2.36E+06	(76)	76.2	58.6	99.1
17	1.00E+07	(330)	3.70E+06	(122)	76.2	61.9	93.9
19	8.01E+06	(271)	2.93E+06	(99)	77.1	61.2	97.1
20	7.13E+06	(175)	2.53E+06	(62)	79.2	59.3	105.7
21	1.50E+07	(331)	5.23E+06	(115)	81.1	65.5	100.3
22	7.84E+06	(232)	2.63E+06	(78)	83.6	64.7	108.0
28	1.76E+07	(387)	5.64E+06	(124)	87.9	71.7	107.7
23	8.05E+06	(293)	2.45E+06	(89)	92.5	73.0	117.3
24	1.03E+07	(157)	3.09E+06	(47)	94.2	67.8	133.4
25	1.37E+07	(312)	4.07E+06	(93)	94.3	74.8	118.9
26	9.31E+06	(197)	2.74E+06	(58)	95.2	71.1	127.3
27	8.35E+06	(212)	2.44E+06	(62)	95.9	72.3	127.0
29	1.64E+07	(263)	4.23E+06	(68)	108.4	83.1	141.3
30	7.54E+06	(236)	1.92E+06	(60)	110.1	83.0	145.9
POOL	9.32E+06	(7216)	3.65E+06	(2827)			

----------PARAMETERS FOR BEST-FIT PEAKS----------

{Standard error for peak age includes group error}
{Peak width is for PD plot assuming a kernel factor = 0.60}

PEAK NUMBER	----PEAK AGE & CONF. INTERVAL (MA)---- MEAN	(----63% CI---)		(----95% CI---)		PEAK WIDTH W(Z)	--GRAINS IN PEAK---- FRAC(%)	SE(%)	COUNT
1)	54.6	(-2.3	+2.4)	(-4.5	+4.9)	0.14	34.0	9.2	10.2
2)	83.6	(-2.8	+2.9)	(-5.4	+5.8)	0.14	66.0	9.2	19.8
						TOTAL:	100.0		30.0